Title

Function of Protein Kinase RNA-like Endoplasmic Reticulum Kinase in regulating tau protein aggregation in Alzheimer's Disease and Progressive Supranuclear Palsy

Author

Xu, Ke

Publication Date

2021

Peer reviewed|Thesis/dissertation

UNIVERSITY OF CALIFORNIA SAN DIEGO

Function of Protein Kinase RNA-like Endoplasmic Reticulum Kinase in regulating tau protein aggregation in Alzheimer's Disease and Progressive Supranuclear Palsy

A Thesis submitted in partial satisfaction for the requirements
for the degree of Master of Science

in

Biology

by

Ke Xu

Committee in charge:

Professor Yimin Zou, Chair
Professor Maho Niwa, Co-Chair
Professor Eric Bennett
Professor Jonathan H. Lin

2021

The thesis of Ke Xu is approved, and it is acceptable in quality and form for publication on microfilm and electronically.

University of California San Diego

2021

DEDICATION

This thesis is dedicated to my parents,

Yongbiao Xu and Li Tang,

for their endless support and love.

This thesis is also dedicated to my friends

who encourage me to go on every adventure.

TABLE OF CONTENTS

LIST OF FIGURES

LIST OF TABLES

LIST OF ABBREVIATIONS

AD	Alzheimer's Disease
PSP	Progressive Supranuclear Palsy
ER	Endoplasmic Reticulum
UPR	Unfolded Protein Response
BiPs	Binding Immunoglobulin Proteins
ATF6	Activating Transcription Factor 6
ATF4	Activating Transcription Factor 4
IRE1	Inositol-Requiring Enzyme 1
PERK	Protein kinase RNA-like Endoplasmic Reticulum Kinase
CHOP	C/EBP Homologous Protein
XBP1	X-box Binding Protein 1
ERAD	Endoplasmic Reticulum-Associated Degradation
ERSE	ER Stress Response Element
MAPT	Microtubule-associated Protein Tau
PHF	Paired Helical Filaments
SF	Straight Filaments
NFT	Neurofibrillary Tangles
Aβ	Amyloid Beta
APP	Amyloid β Precursor Protein

S1P	Site-1 Protease
S2P	Site-2 Protease
GWAS	Genome Wide Association Study
SNP	Single Nucleotide Polymorphism
EIF2AK3	Eukaryotic Translation Initiation Factor 2 Alpha Kinase 3
eIF2α	Eukaryotic translation initiation factor 2 subunit alpha
IPOD	Insoluble Protein Deposit
YFP	Yellow fluorescent protein
TauRD	Tau Repeat Domain

ACKNOWLEDGMENTS

I would like to acknowledge Professor Jonathan H. Lin for his support throughout my entire research journey and for his academic advice. I would also like to thank members of my thesis committee Professor Yimin Zou, Professor Maho Niwa, and Professor Eric Bennett for their sincere advice on my thesis.

I would also like to acknowledge members of Lin Lab especially Dr. GoonHo Park, Dr. Wei Guo, Leon Chea, Lance Sarfarta, and Kyle Kim for their endless support. I appreciate their generous and patient guidance during my research as well as heartful life advice.

The experiments and figures in Chapter 2 were performed/created with Leon Chea. The thesis author was the primary author of this chapter.

The experiments and figures in Chapter 3 were performed/created with Dr. GoonHo Park. The thesis author was the primary author of this chapter.

ABSTRACT OF THESIS

Function of Protein Kinase RNA-like Endoplasmic Reticulum Kinase in regulating tau protein aggregation in Alzheimer's Disease and Progressive Supranuclear Palsy

by

Ke Xu

Master of Science in Biology

University of California San Diego, 2021

Professor Yimin Zou, Chair
Professor Maho Niwa, Co-Chair

Tauopathies, such as Alzheimer's Disease (AD) and Progressive Supranuclear Palsy (PSP), are characterized by the central nervous system accumulation of misfolded tau protein. Endoplasmic reticulum (ER) stress and Unfolded Protein Response (UPR) may be cellular mechanisms that cause tauopathies. As one of three major branches of UPR, PERK was

identified as a genetic risk factor for AD and PSP in several GWAS studies. Upon activation, PERK attenuates protein translation to restore ER homeostasis but prolonged PERK activation can induce apoptosis. Here, we studied the role of PERK in tau aggregation in human AD and PSP brain tissues and in a cell culture model. We prepared protein lysates from the hippocampus region of advanced AD patient brains (Braak 6) and normal brains (Braak 1). We found more tau aggregated protein in Braak 6 brains in comparison to Braak 1 brains by immunoblotting. We also found a statistically significant increase of phosphorylated PERK in Braak 1 brains in comparison to Braak 6 brains in AD patients. This finding suggests that PERK activity is inversely proportional to insoluble misfolded tau aggregation. We did not find any correlation between PERK-haplotype and PERK functional in AD brains. We also prepared protein lysates from 3 different anatomic regions from PSP patient brains (midbrain, frontal cortex, and occipital cortex). The PSP results were highly variable due to technical problems, and we did not identify any reproducible correlations between tau levels and phosphorylated PERK levels.

We further studied how PERK and tau interact utilizing HEK293 cells stably expressing TauRD-YFP (Biosensor cells) developed by Marc Diamond's group as a cellular model of tau protein aggregation. We activated or inhibited PERK activity in TauRD biosensor cells by treating them with pharmacochemical small molecule modulators (GSK2656157, GSK2606414, salubrinal, ISRIB). We monitored tau aggregation by the formation of YFP fluorescent puncta in the cells. We found an inverse association between PERK pathway activation and tau aggregation.

In summary, our brain and cell culture findings implicate PERK as a regulator of tau protein accumulation. PERK pathway activation may have high therapeutic potential for tauopathy treatment.

Chapter 1 Tau expression and PERK analysis in AD

1.1 Introduction

The world population is increasing and aging at an unprecedented pace because of elevated human life expectancy. The elderly population over 65 years old is expected to grow from 551 million in 2010 to more than 2 million by 2050 (Lunenfeld et al., 2013). Aging population comes along with increasing incidences of age-related diseases, especially age-related neurodegenerative diseases (Lunenfeld et al., 2013). Some of these diseases are caused by misfolding, aggregation, and atypical accumulation of a specific toxic protein intra- or extracellularly, which can be termed as proteinopathy (Ghemrawi et al., 2020).

Among proteinopathies, tauopathies are characterized by the central nervous system (CNS) accumulation of misfolded tau protein (Ballatore et al., 2007). Tau is a microtubule-associated protein that promotes axonal stabilization and mediates neuronal activity (Wang et al., 2016). Tau protein is translated from the MAPT gene on chromosome 17. Through alternative splicing mechanisms exerted on exons 2,3 and 10, six different isoforms of tau are expressed in the adult human brain (Espinoza et al., 2008). Three isoforms of tau that contain exon 10 are collectively known as four repeats (4R) tau, and three isoforms that lack exon 10 are collectively known as three repeats (3R) tau (Espinoza et al., 2008). When abnormal post-translational modifications occur, tau proteins undergo atypical phosphorylation and acetylation followed by conformational change; thus, resulting in the formation of neurofibrillary tangles (NFTs) in the cytosol (Ganguly et al., 2017; Saha et al., 2019). NFTs not only sequester functional tau protein, which amplifies the loss of normal function of tau, but also disrupt tau's microtubule-binding ability, obstructing the axonal transport of molecules. Hence, NFTs are considered to be toxic gain-of-function of tau aggregates (Saha et al., 2019). Impediment of axonal transport

subsequently induces neuronal dysfunction and death and deteriorates CNS, phenotypically leading to progressive cognitive and/or motor impairment (Stoothoff et al., 2005). Although more and more evidence support that toxic gains-of-function of tau aggregates contribute to tau-mediated neurodegeneration, the actual mechanism of tau aggregation pathology is still under debate (Wang and Mandelkow, 2016). Because of our limited knowledge of tauopathy, tauopathies have no cure. Understanding the pathogenesis of tauopathy is thus imperative for discovering potential treatments.

Alzheimer's disease (AD) is the most common tauopathy currently affecting around 5.4 million people in the United States; it is expected to affect 1 million new people per year by 2050 (Alzheimer's Association, 2016). AD has an average age of onset around 80 years old and its incidence rate rises markedly with age (Erkkinen et al., 2018). Clinical symptoms of AD include progressive memory loss and visuospatial and executive dysfunction, which is strongly correlated with tau spreading patterns in the brain (Erkkinen et al., 2018). The staging of tau pathology is described as first appearing in the trans-entorhinal region (stages I and II), then spreading to the limbic region (stages III and IV) and neocortical areas (stages V and IV) (Braak and Braak, 1991). The pathological hallmarks of AD are defined by distinct extracellular accumulation of amyloid beta (Aβ) plaque and intracellular accumulation of hyperphosphorylated tau protein known as NFTs. Aβ is a peptide formed by β- and γ-secretase's sequential cleavage of amyloid β precursor protein (APP), a transmembrane protein associated with neuronal development and axonal transport (Kametani and Hasegawa, 2018). In normal conditions, Aβ is cleaved and released outside the cell; however, under pathological conditions, Aβ fails to be degraded and accumulates as Aβ 40 and Aβ 42 due to impaired metabolic activity, leading to neuronal toxicity (Kametani and Hasegawa, 2018). On the other hand, unique paired

helical filaments (PHFs) or straight filaments (SFs) composed of accumulated 3R and 4R tau in hyperphosphorylated state are also distinct pathological inclusions in AD (Kametani and Hasegawa, 2018). Such inclusions are referred to as NFTs if they are formed in neuronal cell bodies or threads if they are formed in dendrites or axons (Kametani and Hasegawa, 2018). The debate over the primary cause of AD between Aβ accumulation and tau lesions has intrigued the field for decades. Currently, there is no disease-modifying treatment for AD, only several FDA-approved drugs for providing cognitive improvement by increasing the amount of neurotransmitter release (Alzheimer's Association, 2020). Previous research focused heavily on Aβ plaque targeting drugs, but these were not successful in the late stage of drug development (Congdon et al., 2018). Other tau- or microtubule-based pharmacological approaches are being studied, such as tau aggregation or acetylation inhibitors; inhibitors of kinases that phosphorylate tau; anti-tau or phosphorylated tau antibodies; microtubules stabilizer; and reduction of tau by antisense oligonucleotides (Wang and Mandelkow, 2016).

Recently, endoplasmic reticulum (ER) stress has emerged in the pathogenesis of tauopathy as various ER stress-associated proteins are identified in post-mortem brain tissues from tauopathy patients along with accumulated NFTs (Hetz et al., 2017). ER is a membrane cellular organelle carrying important functions in synthesis, modification, and transport of membrane and secreted proteins. When misfolded proteins accumulate to a threshold in the ER, the unfolded protein response (UPR) is triggered as an adaptive intracellular signaling pathway (Hoozemans et al., 2005). The chaperone Grp78/immunoglobulin binding proteins (BiPs) thus dissociate from the luminal side of UPR regulator proteins (Hoozemans et al., 2005). The dissociation of BiPs subsequently triggers the activation of UPR regulator proteins including protein kinase RNA-like endoplasmic reticulum kinase (PERK), inositol-requiring enzyme 1α

(IRE1α), and activating transcription factor 6 (ATF6) (Stutzbach et al., 2013). Upon ER stress, PERK activates its cytosolic kinase domain and phosphorylates eukaryotic translational initiation factor 2 alpha subunit (eIF2α), inhibiting translation initiation (Hiramatsu et al., 2015). Reduced translation thus reduces the load of newly synthesized protein that requires ER processing and alleviates ER stress (Hiramatsu et al., 2015). IRE1α is a type I transmembrane protein that contains an endoribonuclease (RNase) domain. Once activated by conformational change due to nucleotide binding, IRE1α's RNase cleaves X-box binding protein-1 (Xbp1) mRNA, leading to upregulation of ER-associated protein degradation (ERAD) factors that enhance ER's protein folding capacity to restore ER homeostasis (Hiramatsu et al., 2015). Different from IRE1α, ATF6 is a type II transmembrane protein that contains a leucine zipper (bZIP) transcription factor. After transiting from the ER to Golgi, ATF6 follows a sequential cleavage by the site-1 and site-2 proteases (S1P and S2P), which activates its bZIP transcriptional activator domain. ATF6 fragments thus migrate to the nucleus to upregulate ERAD components (Hiramatsu et al., 2015). ATF6 also transcriptionally upregulates Xbp1 mRNA level, thereby facilitating the IRE1 pathway.

PERK raised much attention in the neurodegeneration field among the three arms of UPR signaling because it was recently identified as a genetic risk factor associated with tauopathy. Höglinger's team (2011) first discovered an SNP (rs7571971) in EIF2AK3, which encodes PERK, with higher susceptibility towards PSP through a genome-wide association study (GWAS) on PSP patients. Two later studies also confirmed this SNP as risk associated with PSP (Ferrari et al., 2014; Sanchez-Contreras et al., 2018). Then, a follow-up study aiming for AD later revealed the same SNP as linked to the late-onset AD in apolipoprotein E4 (APOE4) cases (Wong et al., 2019). PERK, upon the recruitment by UPR, dimerizes and triggers

phosphorylation of eIF2α on Ser51, inhibiting the guanine nucleotide exchange factor eIF2B (Hiramatsu et al., 2015). As eIF2B is required to covert inactive GDP-bound eIF2 to active GTP bound state, inactive eIF2 complex prevents the formation of the ternary complex (Hiramatsu et al., 2015). Hence, translation initiation is impeded, and protein synthesis is greatly reduced. The less active phosphorylated eIF2α also promotes translation of activating transcription factor 4 (ATF4), which upregulates transcription of genes with a protective effect against oxidative stress (Stutzbach et al., 2013). PERK pathway regulator proteins are also players in autophagy, a process that degrades misfolded proteins (Stutzbach et al., 2013). Nevertheless, prolonged PERK signaling promotes cell death by upregulating the proapoptotic transcriptional factor CHOP, which is downstream of ATF4 (Stutzbach et al., 2013). Thus, PERK can lead to both cytoprotective and proapoptotic response, meaning that a careful regulation of PERK pathway is important for maintaining normal cellular function (Stutzbach et al., 2013).

In the post-mortem human brains of AD patients, there is an increased amount of activated PERK proteins detected, suggesting the possible link between activated PERK proteins and neurodegeneration (Stutzbach et al., 2013; Hoozemans et al., 2005). Pharmacological activation of PERK, achieved by small molecule therapy (Sephin1) or genetic modification, is found to cause a reduction in tau pathology and improvement in cognitive and motor function in the mice model (Yuan et al., 2018). However, pharmacological inhibition of PERK, achieved by inhibitors GSK2606414 or integrated stress response inhibitor (ISRIB), also reduces tau pathology and improves function (Yuan et al., 2018). These studies suggest that modulation of PERK activity can affect tau pathology. If PERK is responsible for regulating tau progression in tauopathy, PERK could serve as a desiring candidate for drug development. Nevertheless, the underlying mechanism behind the PERK pathway and tau progression remains ambiguous.

Furthermore, the human PERK SNP linked to tauopathy is not found in mice. What is the exact circuit intertwining PERK and pathological tau? What is the cause-and-effect relationship between them? How does PERK SNP link to PERK functionality? Understanding the cellular and molecular mechanisms behind the PERK signaling pathway and tau is important in filling the long-existing research gap on tauopathies and achieving the goal of developing a strong disease-modifying treatment for tauopathies.

Therefore, the primary aim of the research in this chapter is to study the role of PERK in the pathogenesis of AD by examining the interplay of tau protein and PERK protein. We utilize western blot to quantify the level of phosphorylated tau over total tau and the level of phosphorylated PERK over total PERK in the hippocampus region of post-mortem AD brains, to determine if there is any significant relationship between the level of tau and PERK in diseased AD state. Moreover, we examine the PERK SNP status of the AD brains to determine if there is an association between PERK SNP and PERK functionality.

1.2 Materials and Method

Brain lysis PHF preparation

Human brain tissues were collected from hippocampus adjacent region from AD patient brains at the UCSD Shiley-Marcos Alzheimer Disease Research Center. Brains were provided to us and homogenized with 10x volume (w/v) Geodert buffer composed of 10mM Tris-HCl, pH = 7.4, 0.8M NaCl, 1mM EGTA, and 10% sucrose. The homogenate mixture was then spun at 20,000xg for 20 minutes. The supernatant was retained afterwards and re-homogenized in 5x volume (w/v) of Geodert buffer. The homogenate was then centrifuged at 20,000xg for 20 minutes and pooled the previous supernatant with the new supernatant. 1% N-Lauroylsarcosine was added and the mixture rocked for 1 hour room temperature. After 1 hour, the mixture was centrifuged for another hour at 100,000xg. Supernatant was discarded at this point and the PHF tau is seen as a dark red-brown pellet and resuspended in 50mM Tris-HCl, pH = 7.5 at 0.2mL of mixture per gram of pellet, then stored at 4°C (Figure 1).

Brain lysis Dephosphorylation preparation

The resuspended sarcosyl-insoluble pellet was brought to a final concentration of 4M with guanidine hydrochloride. The mixture was then dialyzed for 2 hours at 4°C against 50mM Tris-HCl, pH = 7.5. The buffer was changed and dialyzed in new guanidine hydrochloride overnight at 4°C. Then, the sample was centrifuged for about 3-5 minutes and flocculent was removed. The retained supernatant was then dephosphorylated with 20U/µL lambda protein phosphatase. Reaction was stopped by using Laemmli loading buffer and heating (Figure 1).

Western Blots

AD human patient brains were probed with antibodies 1:2000 anti-tau monoclonal MN1000 HT7 (Thermofisher), 1:1000 anti-Phospho-tau (Ser202, Thr205) AT8 (Thermofisher),

1:1000 anti-PERK (C33E10) (Cell Signaling), 1:1000 anti-Phospho-PERK (T982) (abcam), 1:1000 anti-GAPDH (14C10) (Cell Signaling). Membranes were incubated with horseradish peroxidase-coupled secondary antibody (Cell Signaling). After overnight incubation with primary antibody in the cold room, membranes were washed in TBS with 0.1% Tween-20, followed by incubation of a horseradish peroxidase-coupled secondary antibody (Cell Signaling, Danvers, MA). Immunoreactive bands were detected with the SuperSignal West chemiluminescent substrate (Pierce, Rockford, IL).

Statistical Analysis

All the statistics were expressed as mean ± standard error of the mean (SEM). Student's t-test was used for comparison. Two-way ANOVA and Fisher's least significant difference procedure (LSD test) were used to examine the differences among the group of means. All the statistical tests were performed using GraphPad Prism 6. The difference between the means of separate experimental groups was considered statistically significant at $P < 0.05$.

1.3 Results

More phosphorylated tau and total tau are found in Braak 6 brains compared to Braak 1 in AD patients

In AD brains, neurofibrillary tau pathology is observed in multiple brain regions and the progression of tau deposit starts from the entorhinal cortex and later spreads to larger brain areas (Figure 2) (Takeda, 2019). To study the tau expression pattern in AD brains, we used transgenic PS19 mice (PS19 hTau+) as positive control and wild-type PS19 mice (PS19 WT) as negative control for tau protein expression. PS19 hTau+ mice lines are driven by prion promoter overexpressing human 1N4R tau isoform, which includes the P301S tau gene (MAPT) mutation (Iba et al., 2013). We specifically analyzed the hippocampus region of 20 Braak 1 and 20 Braak 6 stage AD patient brains using tau-specific antibodies, AT8 (phosphorylated PHF tau) and HT7 (total tau) (Table 1 and 2).

In the soluble portion of Braak 1 stage AD patient brains, we detected varied amount of total tau protein (HT7+) but no pathologic tau protein (AT8+), with patient 5327 and 5447 expressing a much higher amount of total tau compared to other patients (Figure 3a). Such HT7 level is nearly comparable to PS19 mice overexpressing human tau (hTau+), the positive control (Figure 3a). Similarly, varied amounts of total tau are observed in the insoluble portion of braak 1 stage AD patient brains, especially patient 5386 (Figure 3b).

In the soluble portion of Braak 6 staging of AD patient brains, we observed differential levels of HT7 across patients with patient 5534 most comparable to transgenic PS19 hTau+ (Figure 4a). Compared to the insoluble portion of Braak 1 brains, there were more detectable phosphorylated PHF tau in that of Braak 6 brains, though less than overexpressed human tau in the PS19 mice model (Figure 4b).

When comparing the **soluble** portion of Braak 1 and Braak 6 staging of AD brains, we found a consistent trend in which the level of HT7 and AT8 are similarly varied across patients; such that, there is no significant difference in total tau and phosphorylated PHF tau between the two stages (Figure 5). However, there was a noticeable difference in total tau and phosphorylated PHF tau in the **insoluble** portion that Braak 6 contained more visible HT7 and AT8 expression than Braak 1 when probed (Figure 6).

Less phosphorylated PERK found in Braak 6 brains compared to Braak 1 in AD patients

After determining tau expression, we analyzed expression of total PERK and activated phosphorylated PERK in Braak 1 and Braak 6 brains, to determine if there was any possible linkage between PERK and tau expression. We examined the level of P-PERK (phosphorylated PERK) and T-PERK (total PERK) of Braak 1 and Braak 6 brains. GAPDH is probed as a loading control, confirming equal protein loading. After normalization of P-PERK/T-PERK, we found that Braak 1 staging of AD brains exhibit significantly more P-PERK expression than Braak 6 (Figure 7b). We did not find any association between the Braak staging, PERK haplotype, and PERK protein expression (Figure 7a). Finally, we also did not detect any P-PERK and T-PERK expression in the insoluble portion of these brains.

1.4 Discussion

Tau deposition is associated strongly with cognition and AD pathology (Schöll et al., 2019). Tau distribution pattern in the AD brain starts in the entorhinal cortex (Braak stage I/II) and spreads through temporal lobes and medial parietal lobes (Braak stage III/IV) to wide areas of the neocortex (Braak stage V/VI) (Schöll et al., 2019). Soluble, intracellular tau pretangles first appear at the locus coeruleus and other brainstem nuclei and then spread to the transentorhinal cortex. At the transentorhinal cortex, insoluble NFTs begin to accumulate and spread to hippocampus and entorhinal cortex, finally following the spreading pattern (Braak and Braak, 1991). In order to study the tau deposit pattern in AD brains to confirm previous findings, we utilized Goedert PHF dispersion preparation protocol that uses specific antibodies to distinguish tau isoforms and label PHFs (Goedert et al., 1992). With modification made by Rohan de Silva, we were able to obtain bands on western blots that represented phosphorylated (AT8) and non-phosphorylated tau (HT7). Consistent with previous findings, we found similar protein levels of tau regardless of braak staging in the soluble portion of brain lysates and higher level of total tau in Braak 6 compared to Braak 1 staged brains (Figure 3,4 and 5). Moreover, we found significantly more total tau in Braak 6 compared to Braak 1 staged brains in the insoluble portion of our brain lysates (Figure 6). This is also consistent with the fact that the amount of insoluble fibers of NFTs increases with the severity of Braak staging such that Braak 1 has the least amount of insoluble tau and Braak 6 has the most amount of insoluble tau.

When examining the P-PERK as well as T-PERK level in AD brains, we found a significantly lower amount of P-PERK relative to total P-PERK in the soluble portion in Braak 6 staged brains compared to Braak 1 staged brain (Figure 7a and 7b). This finding is contradictory to a previous published finding stating that the level of activated PERK (P-PERK) rises with the

level of tau pathology (Stutzbach et al., 2013; Wong et al., 2019). However, both of those studies used immunohistochemistry labeling to examine P-PERK expression on AD brain tissue sections, different from our current study using immunoblotting of hippocampal protein lysates. Nevertheless, a previous finding indicates that tauopathy-associated PERK alleles were found to have reduced kinase activity in response to ER stress, leading to the hypothesis that PERK activity prevents tauopathy (Yuan et al., 2018). Our study matches this hypothesis; it is possible that as AD develops, P-PERK protein level decreases and this leads to the increase in tau level in the Braak 6 brains (Figure 5 and 7). Lowered kinase activity of PERK could increase tau protein translation leading to tau aggregation and the deterioration of the disease.

When we tried to detect P-PERK or total PERK in the insoluble portion of AD brains lysate (Figure 7c), we failed to detect any PERK protein. This indicates that PERK is likely not part of the tau aggregates that accumulate in the insoluble protein fractions. Besides regulating tau translation, PERK activity could be linked to AD pathology through an alternative pathway. In yeast, misfolded protein and prion protein are specifically directed to insoluble protein deposit (IPOD) site, where cell initiates biogenesis of autophagosomes, by an actin-based transport machinery for degradation or refolding (Rothe et al. 2018). As PERK is also a player in autophagy, it is possible that PERK somehow affect the autophagy process to regulate tau progression. However, such a very early postulation needs extensive further studies to validate. Future studies can be focused on dissecting more PERK-related downstream pathways to gain a thorough understanding of the differential relationship of PERK and tau in these conditions so that we may have a clearer idea about which PERK-regulated pathways are most likely involved in the pathogenesis of tauopathy.

1.5 Figures and Table

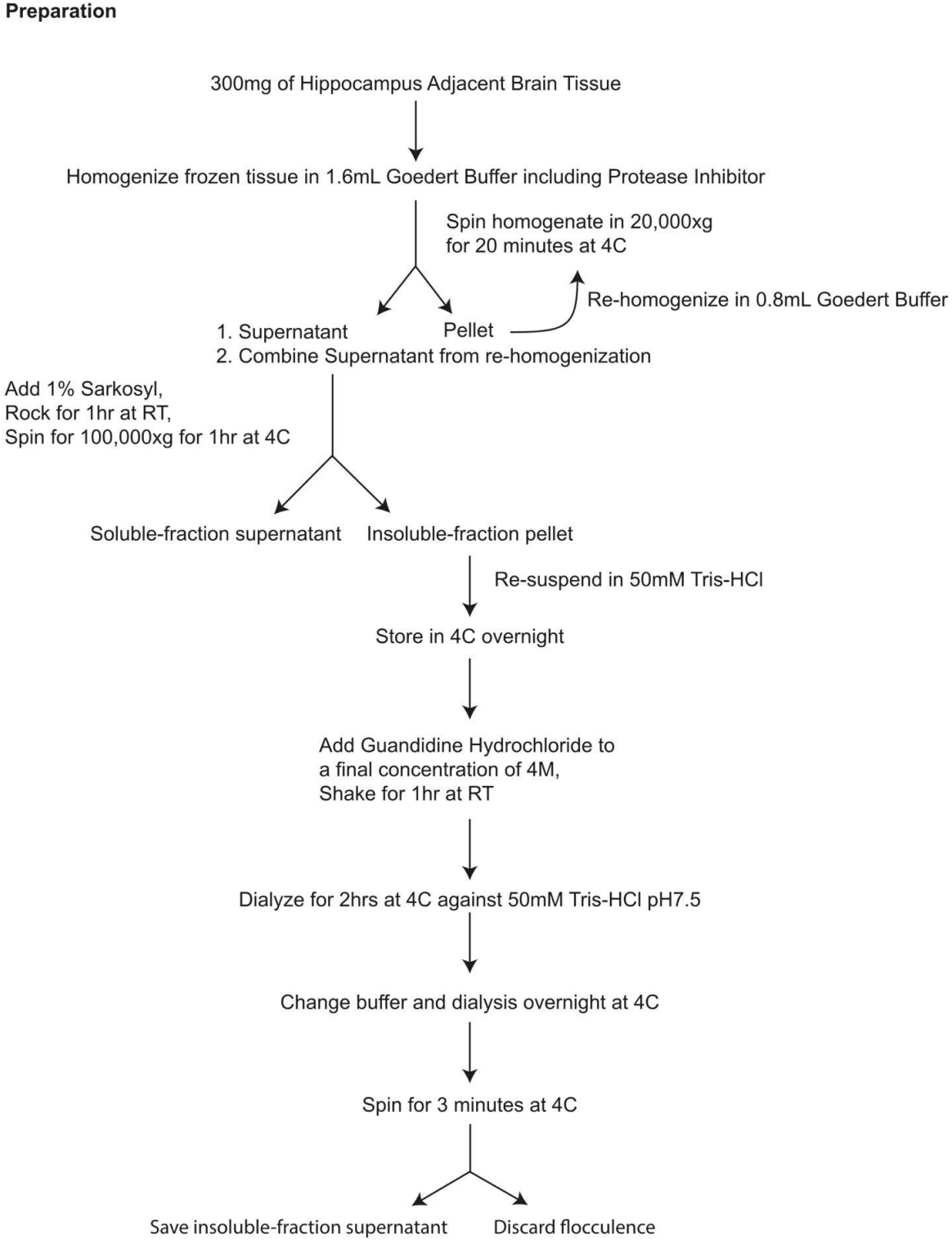

Figure 1. Brain Lysis PHF preparation protocol.

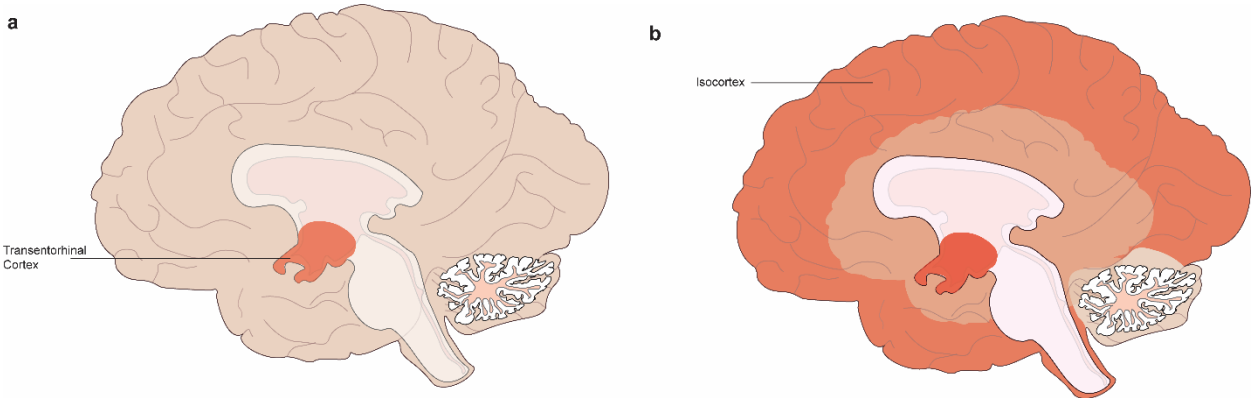

Figure 2. Concentration of tau over-time in AD brains

(a) Diagram of Braak 1 patient brain with concentration of tau indicated in red. (b) Diagram of Braak 6 patient brain with concentration of tau spread throughout the rest of isocortex and in transentorhinal region.

Table 1. AD Patient Braak 1 Brain Information

Gender and age of Braak 1 patient brains. Information on two PERK allele SNP variants Rs867529 and Rs1805165. Patient PERK haplotype information.

Patient ID	Gender	Age	Rs867529 (C/G) TCC → TGC S136C	Rs1805165(T/G) TCT → GCT S704A	Haplotype
5529	M	81	C/G	T/G	AB
5517	M	86	C/G	T/G	AB
5515	F	73	TGC	GCT	BB
5510	M	92	TCC	TCT	AA
5501	F	86	C/G	T/G	AB
5499	M	76	TCC		AA
5490	M	87	TCC	TCT	AA
5459	M	68			
5455	F	93	TCC		AA
5452	M	83	G/C	T/G	AB
5447	F	91	G/C	T/G	AB
5422	M	90	TCC	TCT	AA
5421	M	86	TGC	TCT	AA
5412	M	73	TCC	TCT	AA
5399	M	92	TCC	TCT	AA
5386	M	74			
5372	F	84	C/G	T/G	AB
5356	M	79			
5353	M	78	TCC	TCT	AA
5327	M	94	TCC	TCT	AA

Table 2. AD Patient Braak 6 Brain Information

Gender and age of Braak 6 patient brains. Information on two PERK allele SNP variants Rs867529 and Rs1805165. Patient PERK haplotype information.

Patient ID	Gender	Age	Rs867529 (C/G) TCC → TGC S136C	Rs1805165(T/G) TCT → GCT S704A	Haplotype
5596	M	55	TCC	TCT	AA
5595	M	76	TCC	TCT	AA
5593	M	74			
5586	F	77	G/C		AB
5585	F	68	G/C	T/G	AB
5581	F	64	G/C	T/G	AB
5569	F	87	G/C	T/G	AB
5566	F	84		TCT	AA
5565	F	55			
5560	F	83	G/C	T/G	AB
5559	F	86			
5557			G/C	T/G	AB
5556	M	76	TCC	TCT	
5555	M	56			
5554	M	71	TCC	TCT	AA
5548	M	80	G/C	T/G	AB
5543	M	92	TCC	TCT	AA
5537	F	65	G/C	GCT	BB
5534	F	100	TGC	GCT	BB

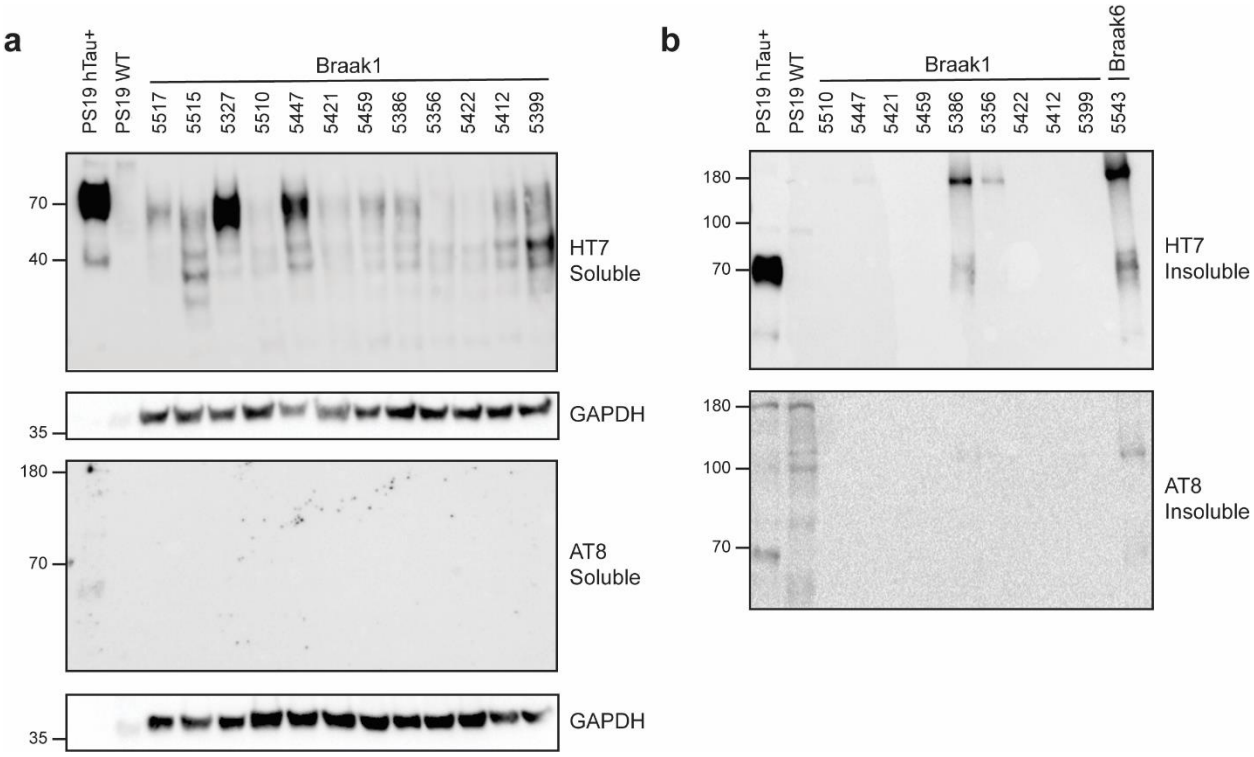

Figure 3. ADRC AD Braak1 (Normal) Brains Do Not Express Misfolded Phosphorylated Pathologic Tau (AT8-negative)

(a) Western blot of soluble brain lysates from PS19 transgenic hTau+ mice (positive control), PS19 WT mice (negative control), and Braak 1 AD brains probed with total human tau (HT7) and phosphorylated human tau (AT8). (b) Western blot of insoluble brain lysates from PS19 transgenic hTau mice, PS19 WT mice, and Braak 1 AD brains probed with HT7 and AT8.

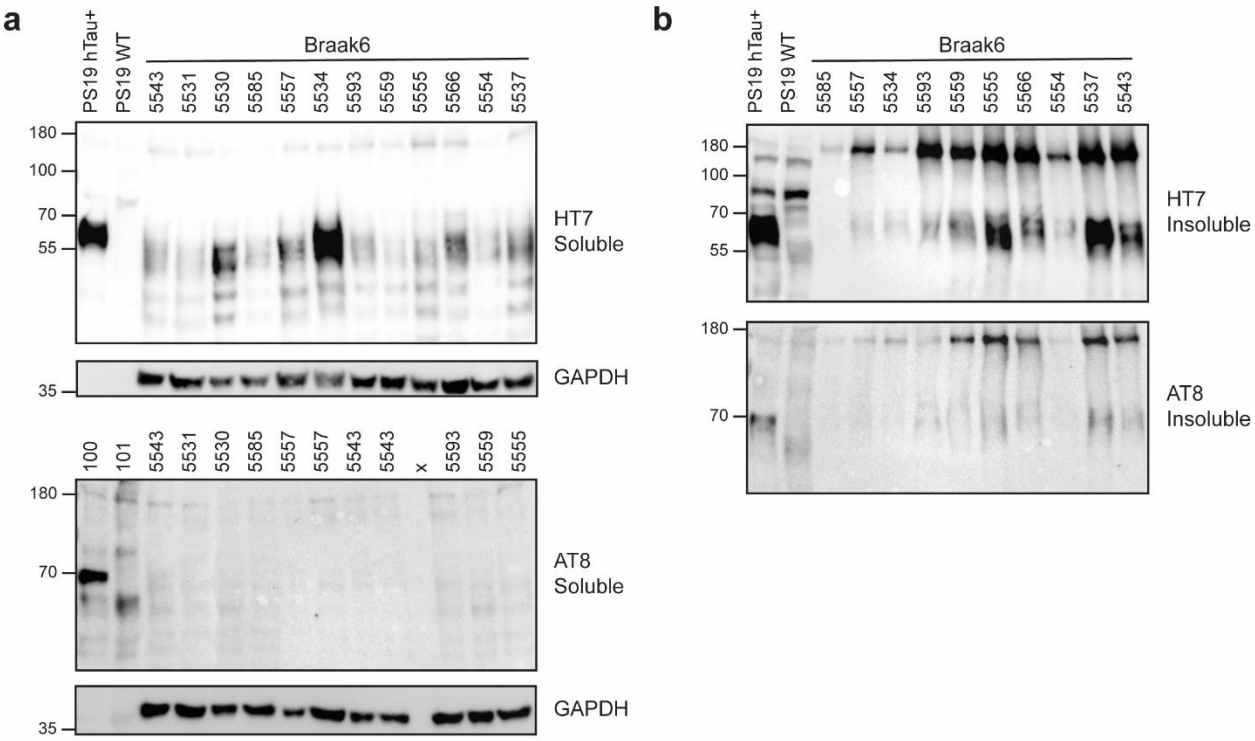

Figure 4. ADRC AD Braak6 Brains Express Misfolded, Phosphorylated Pathologic Tau (AT8-positive)

(a) Western blot of soluble brain lysate from PS19 transgenic hTau+ mice (positive control), PS19 WT mice (negative control), and Braak 6 AD brains probed with HT7 and AT8. (b) Western blot of insoluble brain lysate from PS19 transgenic hTau+ mice, PS19 WT mice, and Braak 6 AD brains probed with HT7 and AT8.

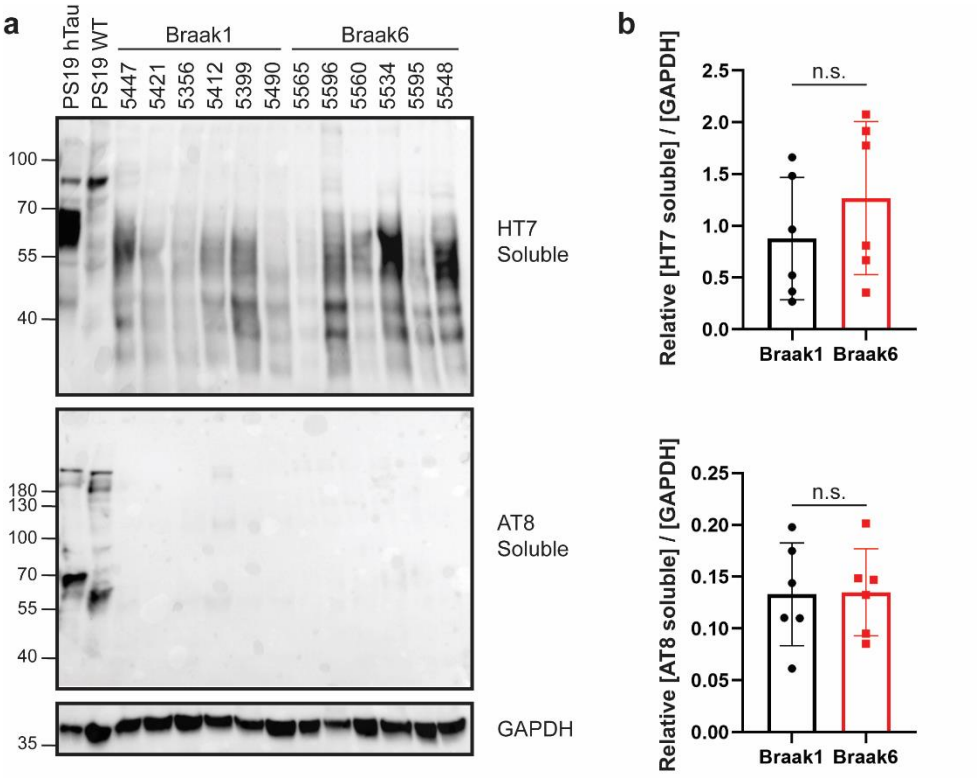

Figure 5. Total tau (HT7) and phosphorylated tau (AT8) levels do not differ between ADRC AD Braak1 and Braak 6 brains in the soluble fraction

(a) Comparison western blot of soluble brain lysates from PS19 transgenic hTau+ mice (positive control), PS19 WT mice (negative control), and AD brains probed with HT7 and AT8. GAPDH used as loading control. (b) Quantified graph of soluble HT7 normalized over GAPDH and soluble AT8 normalized over GAPDH of Braak 1 and Braak 6 AD patient brains. Data were analyzed by Student's t-test and showed significance at $*P < 0.05$.

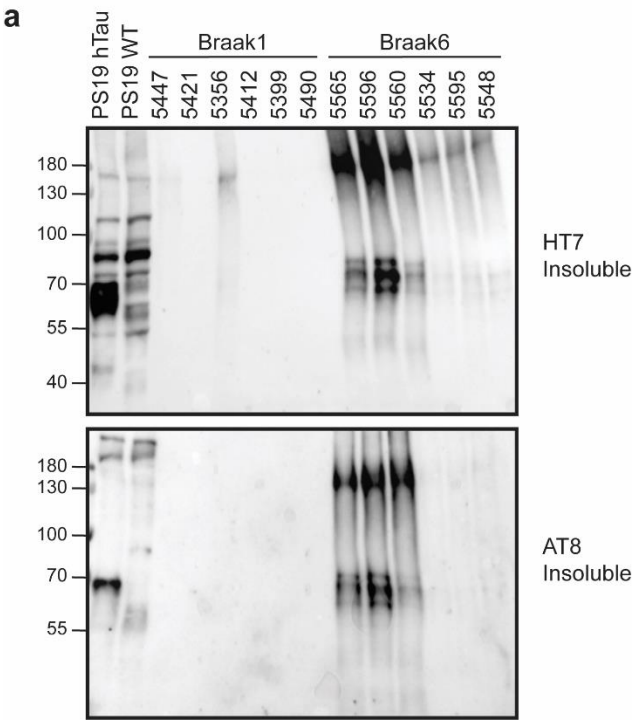

Figure 6. Braak6 Brains have much more total tau (HT7) and pathologic tau (AT8) compared to Braak 1 Brains in the Insoluble fraction

(a) Comparison western blot of insoluble brain lysates from PS19 transgenic hTau+ mice (positive control), PS19 WT mice (negative control), and AD brains probed with HT7 and AT8.

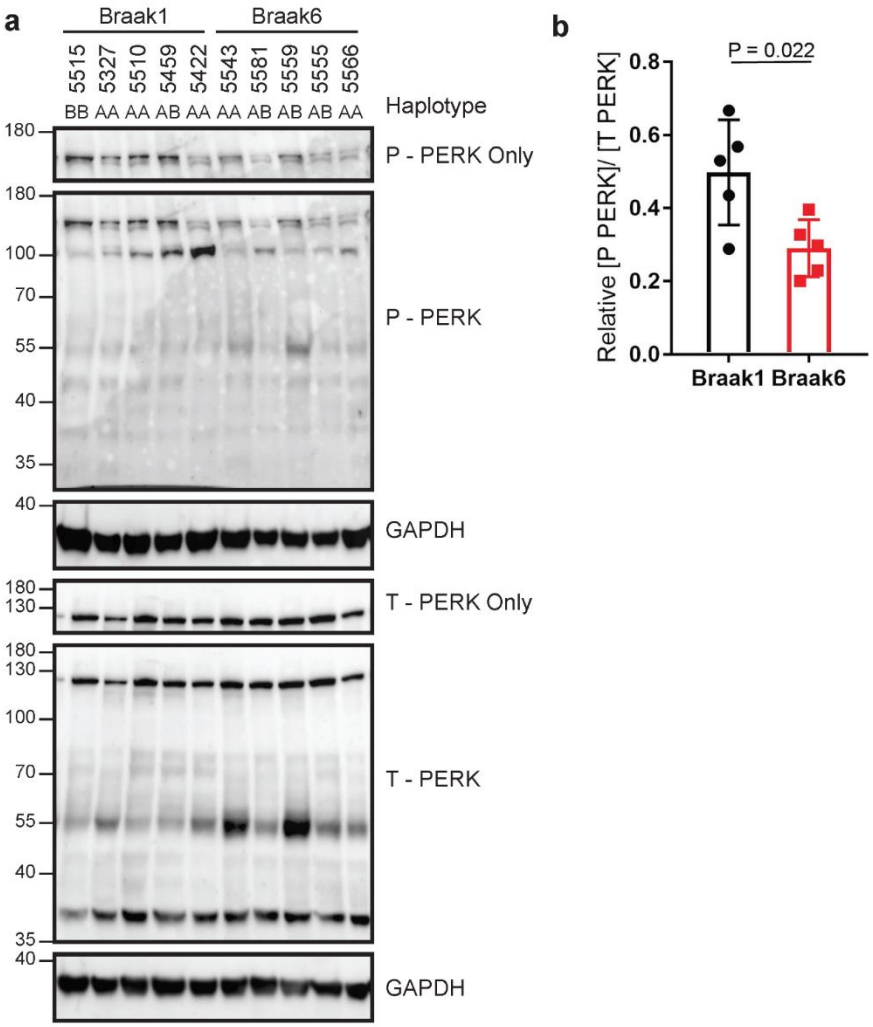

Figure 7. P-PERK levels are increased in Braak 1 Brains compared to Braak 6 Brains
(a) Comparison western blot of soluble brain lysates probed with P PERK and T PERK. GAPDH used as control. Haplotype information corresponds to Braak 1 or Braak 6 patients. (b) Quantified graph illustration of relative P PERK concentration normalized to T PERK. Data were analyzed by Student's t-test and showed significance at $*P < 0.05$

Chapter 2 Tau expression and PERK analysis in PSP

2.1 Introduction

Progressive supranuclear palsy (PSP), also known as Steele-Richardson-Olszewski syndrome, is a relatively rare 4R-tauopathy sharing similar pathology with AD by its characteristic intracellular NFTs composed of hyperphosphorylated tau. Neuropathological evidence identifies NFTs affecting a wide range of brain areas in PSP, including the basal ganglia, brain stem, and cerebellum, areas subjected to neuronal cell loss and gliosis. When midbrain atrophy is severe, it shows up as the typical "hummingbird sign" on MRI (Erkkinen et al., 2018). PSP has an incidence rate around 1.4 to 6.4 individuals per 100,000, rising with age (Erkkinen et al., 2018). It is an atypical Parkinsonian disorder associated with progressive motor impairment and cognitive decline with an average age at death around 75 years and an average disease duration of 7 years (Dickson et al., 2007). There are many PSP subtypes identified according to tau pathological load differences. Diagnosis of PSP is based on the presence of neurofibrillary tangles and threads in neurons, coiled bodies in oligodendroglia and tufts in astrocytes ("tufted astrocytes") in affected brain regions (Sakae et al., 2019; Kovacs et al., 2020). Tau progression in PSP usually begins at the subcortical and brainstem nuclei followed by accumulation in the neocortical region of the brain (Kovacs et al., 2020). There is currently no cure for the disease while some treatments can improve the balance and gait or speech generation (Erkkinen et al., 2018).

Recently, much attention has been attracted to PERK as having therapeutic potential in treating PSP and tauopathies with shared pathogenicity. The Höglinger team (2011) first identified eukaryotic translation initiation factor 2 alpha kinase 3 (EIF2AK3), which encodes PERK, as a genetic risk locus for PSP in genome-wide association study. Based on this finding,

other groups later identified two functional haplotypes associated with the human EIF2AK3 locus-haplotype A (Ser136-Arg166-Ser704) and haplotype B (Cys136-Gln166-Ala704); both are generated by tauopathy-associated single nucleotide polymorphism (SNP) (Ferrari et al., 2014; Sanchez-Contreras et al., 2018). There are four SNPs variants on PERK in total linked to tauopathy, including rs7571971 that is in the intronic region of PERK and rs867529, rs13045, rs1805165 that are in the coding region of PERK (Höglinger et al., 2011; Ferrari et al., 2014; Sanchez-Contreras et al., 2018). The haplotype A and B contain major and minor alleles for the four SNPs respectively; major allele is disease-protective while minor allele increases risk of disease (Yuan et al., 2018). There are also another rare SNP (rs55791823) in the coding region of EIF2AK3 with minor allele frequency of 0.016 that is predicted to be disease-linked. Although more genetic studies confirmed that PERK haplotype is genetically associated with increased PSP risk, it is unclear how PERK is involved in the pathogenesis of PSP (Stutzbach et al., 2013).

Therefore, the experimental aim of this chapter is to understand the relationship between PERK function and tau in PSP. To achieve this aim, we utilize western blot to quantify the level of total tau, phosphorylated tau protein, total PERK, phosphorylated PERK protein in human PSP brains. Since pathological NFTs accumulation in PSP brains follows a midbrain to fronto-parietal to occipital sequence, we specifically did western blotting on protein lysates from the frontal cortex, occipital cortex and midbrain region of PSP patients' brains to see if there was any relationship between tau and PERK protein expression (Kovacs et al., 2020). We also examined the PERK haplotypes of these PSP brains in the study to understand whether there is an association between PERK haplotypes and PERK function in PSP brain pathology.

2.2 Materials and Method

Brain lysis PHF preparation

Human brain tissues were collected from midbrain, occipital, and frontal cortex region from PSP brains, provided by Rohan de Silva, DPhil from UCL Queen Square Institute of Neurology and London. Brains were provided to us and homogenized with 10x volume (w/v) Geodert buffer composed of 10mM Tris-HCl, pH = 7.4, 0.8M NaCl, 1mM EGTA, and 10% sucrose. The homogenate mixture was then spun at 20,000xg for 20 minutes. The supernatant was retained afterwards and re-homogenized in 5x volume (w/v) of Geodert buffer. The homogenate was then centrifuged at 20,000xg for 20 minutes and pooled the previous supernatant with the new supernatant. 1% N-Lauroylsarcosine was added and the mixture rocked for 1 hour room temperature. After 1 hour, the mixture was centrifuged for another hour at 100,000xg. Supernatant was discarded at this point and the PHF tau is seen as a dark red-brown pellet and resuspended in 50mM Tris-HCl, pH = 7.5 at 0.2mL of mixture per gram of pellet, then stored at 4°C (Figure 1).

Brain lysis Dephosphorylation preparation

The resuspended sarcosyl-insoluble pellet was brought to a final concentration of 4M with guanidine hydrochloride. The mixture was then dialyzed for 2 hours at 4°C against 50mM Tris-HCl, pH = 7.5. The buffer was changed and dialyzed in new guanidine hydrochloride overnight at 4°C. Then, the sample was centrifuged for about 3-5 minutes and flocculent was removed. The retained supernatant was then dephosphorylated with 20U/µL lambda protein phosphatase. Reaction was stopped by using Laemmli loading buffer and heating (Figure 1).

Western Blots

PSP human patient brain protein lysates were probed with antibodies 1:2000 anti-tau monoclonal MN1000 HT7 (Thermofisher), 1:1000 anti-Phospho-tau (Ser202, Thr205) AT8 (Thermofisher), 1:1000 anti-PERK (C33E10) (Cell Signaling), 1:1000 anti-Phospho-PERK (T982) (abcam), 1:1000 anti-GAPDH (14C10) (Cell Signaling). Membranes were incubated with horseradish peroxidase-coupled secondary antibody (Cell Signaling). After overnight incubation with primary antibody in the cold room, membranes were washed in TBS with 0.1% Tween-20, followed by incubation of a horseradish peroxidase-coupled secondary antibody (Cell Signaling, Danvers, MA). Immunoreactive bands were detected with the SuperSignal West chemiluminescent substrate (Pierce, Rockford, IL).

Statistical Analysis

All the statistics were expressed as mean ± standard error of the mean (SEM). Student's t-test was used for comparison. Two-way ANOVA and Fisher's least significant difference procedure (LSD test) were used to examine the differences among the group of means. All the statistical tests were performed using GraphPad Prism 6. The difference between the means of separate experimental groups was considered statistically significant at $P < 0.05$.

2.3 Results

No phosphorylated tau in PSP Frontal Cortex brains

Pathological tau accumulation as NFTs in PSP brains following a midbrain to fronto-parietal to occipital cortex anatomic distribution (Kovacs et al., 2020). The most tau accumulates in the midbrain, and the forebrain and occipital cortex have less tau (Figure 8) (Kovacs et al., 2020). To confirm such pathological pattern, we analyzed PSP frontal cortex brains with same method we used for analyzing AD brains. We obtained ten patient brains from Rohan de Silva, DPhil from UCL Queen Square Institute of Neurology and London (Table 3). We used two AD Braak 6 brains as controls to AT8 and HT7 expression. In the PSP frontal cortex soluble protein lysates, HT7 varied between all patients while AT8 was not detectable (Figure 9a). The insoluble portion of the frontal cortex PSP brain lysates showed no presence of total tau and phosphorylated PHF tau (Figure 9b).

Likewise, we also studied the P-PERK and T-PERK expression in PSP frontal cortex brains. Soluble P-PERK protein levels fluctuated among each PSP patient (Figure 9c). When normalizing individual P-PERK expression over T-PERK, there was no indication of any significant difference among PSP patients (Figure 9d).

No detection of phosphorylated tau or phosphorylated PERK in PSP Occipital Brains

Next, we wanted to examine pathological tau expression in PSP occipital brain regions. We used the same ten patient brains from Rohan de Silva, DPhil from UCL Queen Square Institute of Neurology and London (Table 3). The same method mentioned above for the frontal cortex was utilized. We found varied amount of HT7 across soluble portions of multiple PSP patients' brains (Figure 10a). After normalization over GAPDH, expression of soluble HT7 remained varied greatly between PSP patients in comparison to Braak 1 (negative control) and

Braak 6 brains (positive control) (Figure 10c). Unfortunately, we were unable to identify and quantify P-PERK from the PSP occipital brain lysates (Figure 10a). This is likely due to technical experimental problems because our positive ADRC Braak 6 brain lysates also showed no P-PERK when we analyzed the PSP occipital lysates. Finally, we did not detect any HT7 and AT8 from the insoluble portions of PSP occipital brains (Figure 10b).

No detection of any protein by any antibody in PSP Midbrain Cortex brains

Last, we examined PSP midbrain protein lysates in our study (Kovacs et al., 2020). We used the midbrains from the same ten patient brains from Rohan de Silva, DPhil from UCL Queen Square Institute of Neurology and London (Table 3). We employed the same method towards analyzing this brain area. However, we failed to detect any signals from any of our blots (Figure 11). In reviewing our experimental protocol to make protein lysates from brain tissues, we realized that we did not add protease inhibitor cocktail. This error in protein lysis preparation might lead to such failure because the tau and PERK proteins could be degraded without the protease inhibitors.

2.4 Discussion

PSP is a 4R-tauopathy characterized by neurofibrillary tangles composed of hyperphosphorylated tau in subcortical nuclei and the presence of tufted astrocytes. Tau progression in PSP begins at the midbrain and brainstem nuclei followed by accumulation in the neocortical region of the brain (Kovacs *et al.*, 2020). In order to confirm tau expression patterns in different brain regions of PSP as previous findings, we received PSP patients' brains in frontal cortex, occipital and midbrain regions from Rohan de Silva, DPhil from UCL Queen Square Institute of Neurology and London. Like our AD study, we utilized Goedert PHF dispersion preparation protocol that uses specific antibodies to distinguish tau isoforms and label PHFs (Goedert et al., 1992). With modification made by Rohan de Silva, we were able to obtain bands on western blots that represented phosphorylated (AT8) and non-phosphorylated tau (HT7). We found the frontal cortex region of PSP patient brains expressed soluble HT7 but no AT8. Also, there was no HT7 and AT8 in the insoluble frontal cortex PSP brain lysates. This confirmed that the frontal cortex in PSP was not a region of phosphorylated tau aggregation (Figure 9a and 9b). In the occipital region of PSP patient brains, insoluble HT7 and AT8 is not detected while the total tau level in the soluble fraction of occipital regions was comparable (Figure 10). This confirmed that the occipital cortex in PSP was also not a region of phosphorylated tau aggregation. The midbrain immunoblot studies were not successful because we had technical problems preparing protein lysates from the midbrain tissues.

In terms of analyzing the relationship between PERK haplotypes and PERK functionality in PSP, we observe similar total PERK protein expression between non-risk Haplotype A and risk Haplotype B in frontal cortex and occipital region of PSP brain, indicating

no specific correlation between PERK haplotype and PERK protein levels (Figure 9d and 10a). This suggests that PERK haplotype does not alter PERK protein levels in these 2 brain regions.

Unfortunately, we failed to capture any protein from the midbrain region of the PSP brain (Figure 11). It is possible that we forgot to add the specific protease for preventing the degradation of proteins, causing all proteins to degrade. As a result, no matter what antibodies we used for the probe, we were unable to detect any protein. This experimental failure prevents us from reaching any conclusions about tau and PERK protein expression in the PSP midbrain regions.

To conclude, we replicated prior studies that showed little to no phosphorylated tau in frontal cortex and occipital cortex of PSP patients. We find no correlation between PERK haplotypes and PERK protein levels in these two brain regions. Further replicative studies are needed to fix experimental error and more studies should be placed on understanding PERK haplotypes feature in triggering tauopathy.

2.5 Figures and Table

Table 3. PSP Patient Information

Table information on Rs7571971 (C/T) intronic mutation and haplotype relative to PSP patient brains.

Patient ID	Rs7571971 (C/T) Intronic	Haplotype
P33/03	C/C	AA
P33/04	C/C	AA
P12/08	C/C	AA
P21/02	C/C	AA
P47/01	C/C	AA
P67/11	T/T	BB
P62/12	T/T	BB
P56/15	T/T	BB
P63/16	T/T	BB
P66/13	T/T	BB

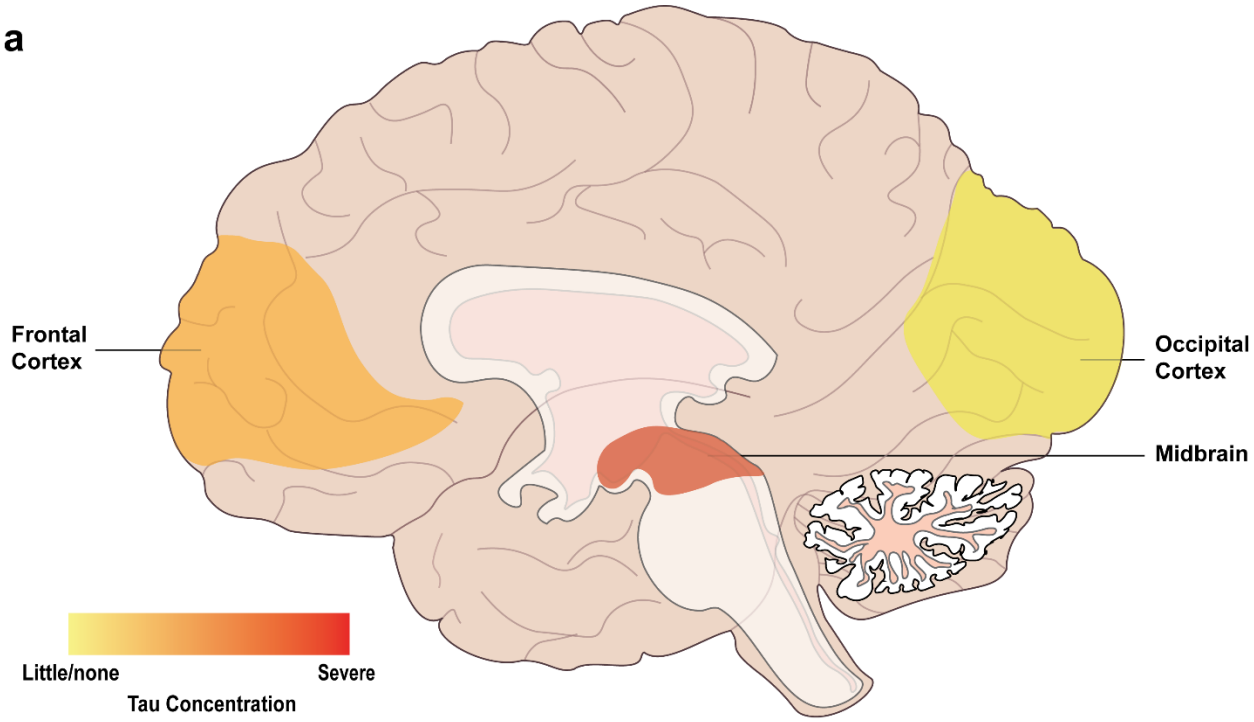

Figure 8. Tau aggregation in PSP brains

Lateral view of a human brain showing areas of low tau deposits (yellow), intermediate (orange), and increased tau aggregation (red).

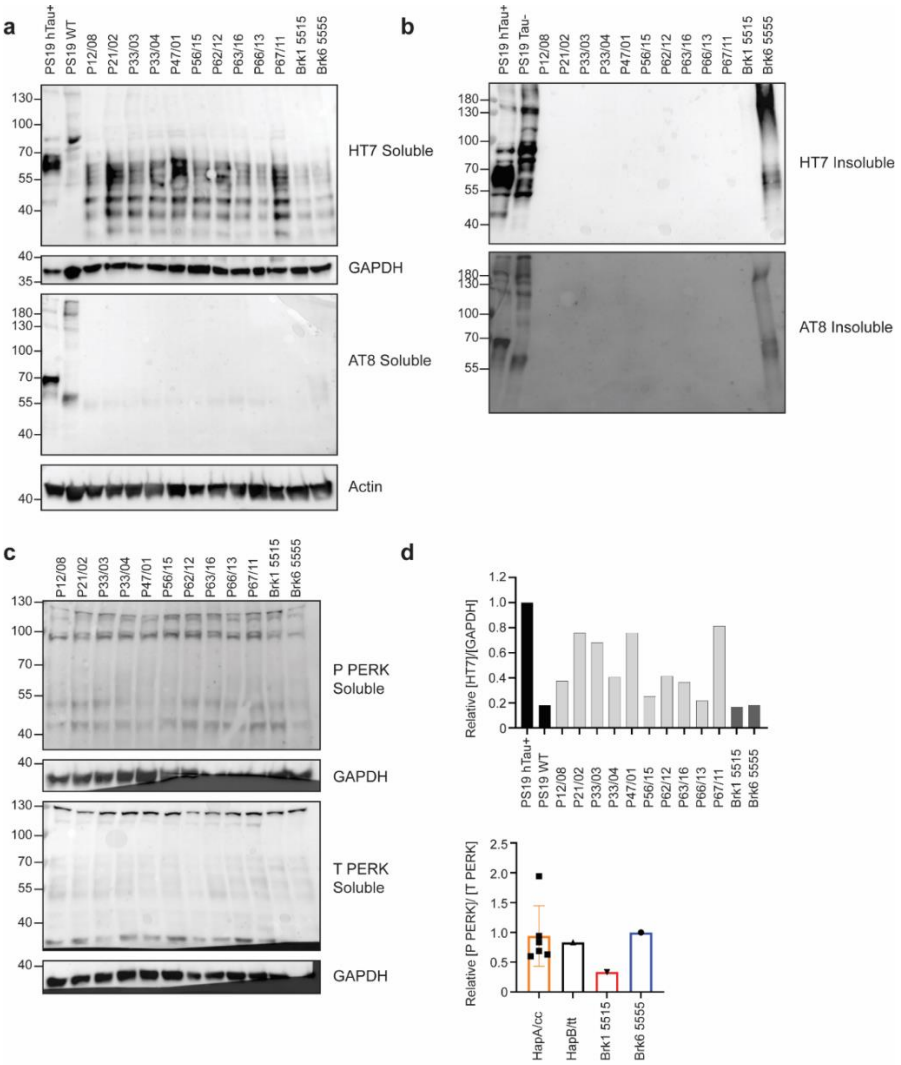

Figure 9. Tau and PERK protein expression in Frontal Cortex PSP Brains Lysates

(a) Western blot of soluble portion of frontal cortex of PSP patient brains probed with HT7 and AT8. GAPDH used as loading control. (b) Western blot of insoluble portion of frontal cortex of PSP brains probed with HT7 and AT8. (c) Western blot of soluble portion of frontal cortex of PSP patient brains probed with P PERK and T PERK. GAPDH used as loading control. (d) Quantified graph of relative HT7 soluble normalized over GAPDH and P PERK normalized over T PERK of soluble PSP patient brains. Data were analyzed by Student's t-test and showed significance at $*P < 0.05$.

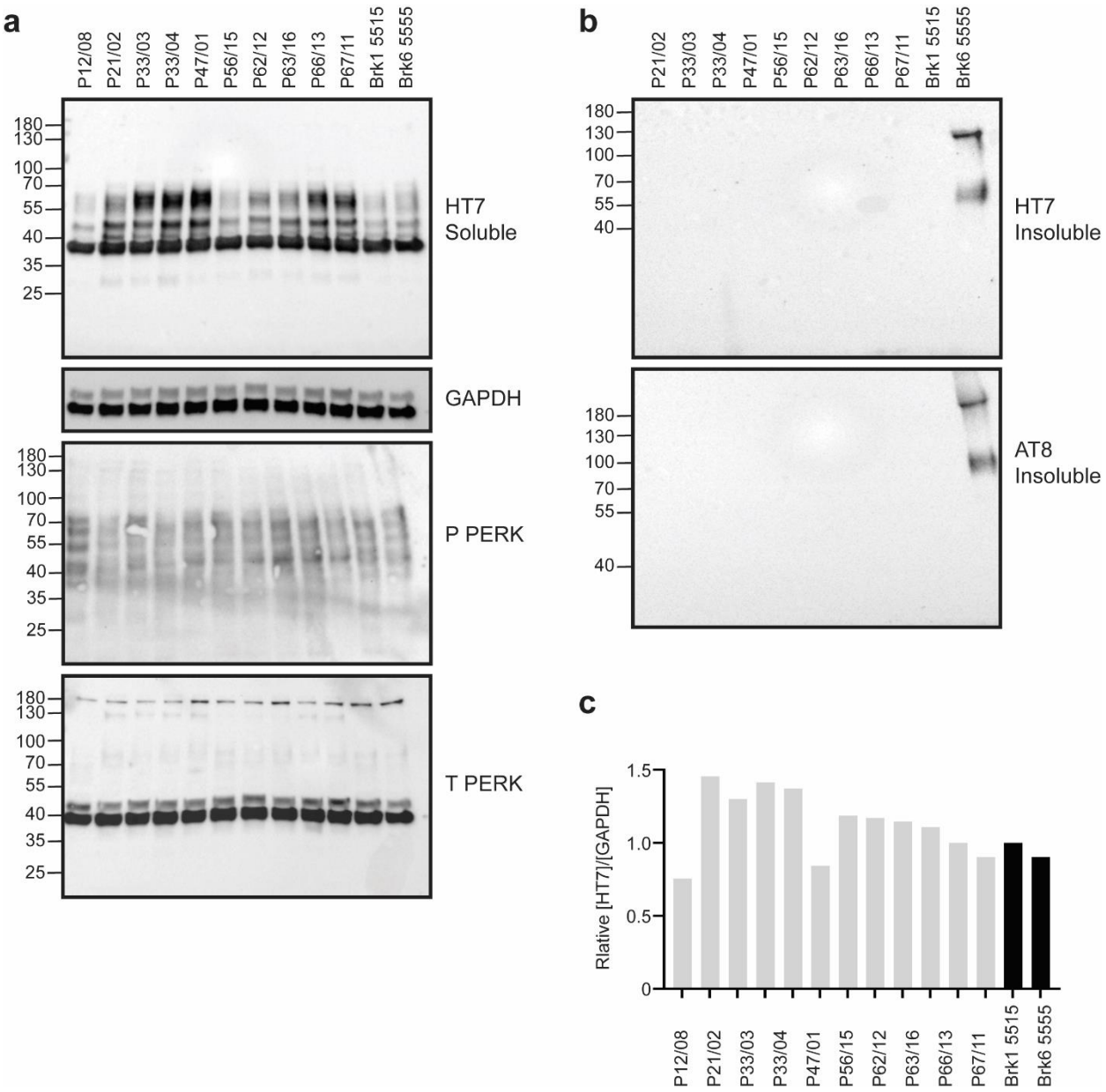

Figure 10. Tau and PERK protein expression in Occipital Cortex PSP Brains lysates

(a) Western blot of soluble portion of occipital cortex of PSP patient brains probed with HT7, P PERK, and T PERK. GAPDH used as loading control. (b) Western blot of insoluble portion of occipital cortex of PSP brains probed with HT7 and AT8. (c) Quantified graph of relative HT7 soluble normalized over GAPDH of soluble PSP patient brains. Data were analyzed by Student's t-test and showed significance at $*P < 0.05$.

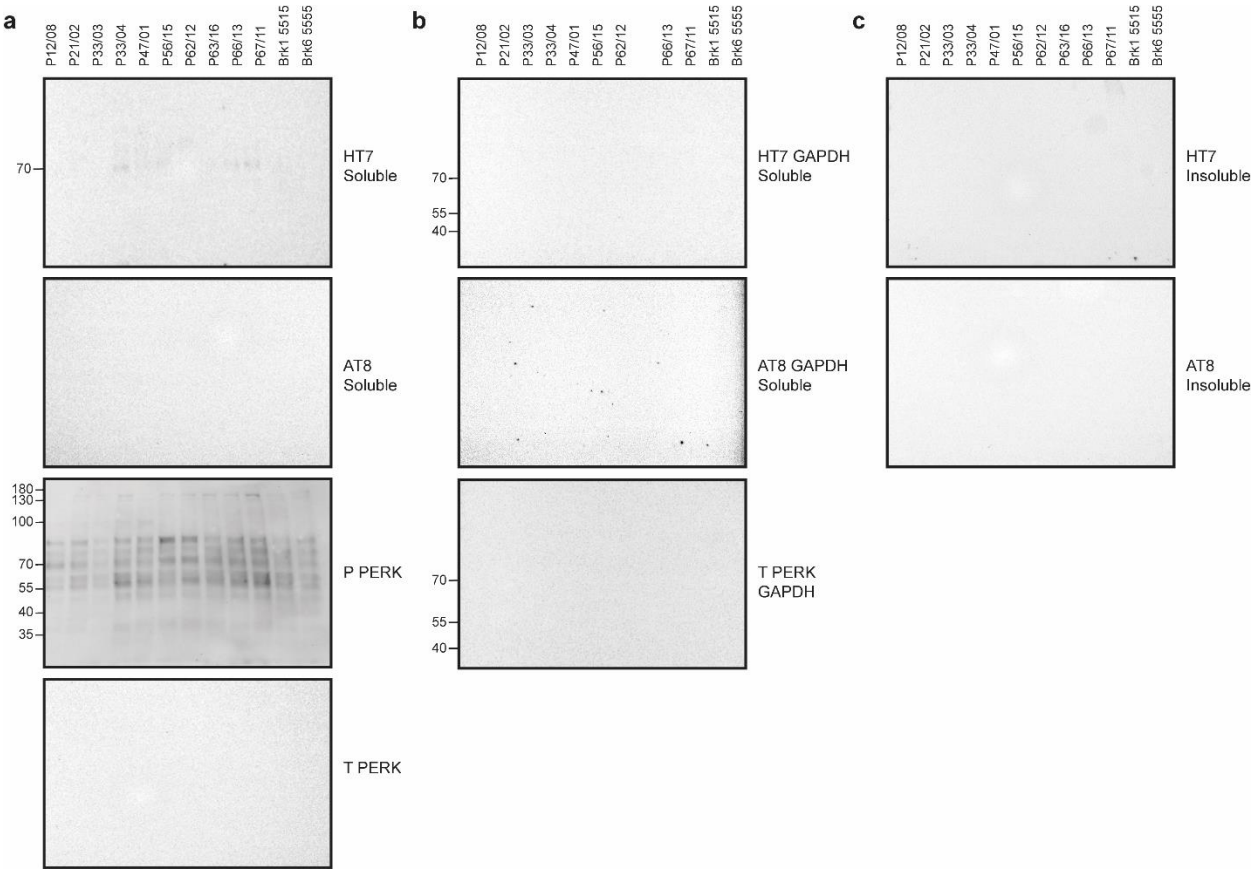

Figure 11. Tau and PERK protein expression in Midbrain Region PSP Brains Lysates
(a) Western blot of soluble portion of midbrain cortex of PSP patient brains probed with HT7, AT8, P PERK, and T PERK. (b) Western blot of soluble portion of midbrain cortex of PSP patient brains probed with GAPDH used as loading control relative to HT7, AT8, and T PERK blots, respectively. (c) Western blot of insoluble portion of midbrain cortex of PSP brains probed with HT7 and AT8.

The experiments and figures in Chapter 2 were performed/created with Leon Chea. The thesis author was the primary author of this chapter.

Chapter 3 Modulation of PERK activity affects tau seeding activity in TauRD-YFP biosensor cells

3.1 Introduction

Recent studies in mouse focusing on pharmacochemical modulation of PERK offer insights into the possible involvement of PERK in the pathogensis of tauopathies. To be specific, pharmacological activation of PERK, achieved by small molecule therapy (Sephin1) or genetic modification, was found to cause reduction in tau pathology and improvement in cognitive and motor function in the mice model (Yuan et al., 2018). Similarly, pharmacological inhibition of PERK, achieved by inhibitors GSK2606414 or ISRIB, led to an identical scenario (Yuan et al., 2018). Moreover, increased level of total tau and pathological phosphorylated tau were detected in iPSC-derived neurons carrying tauopathy-associated *PERK* variants during ER stress or after PERK GSK inhibition treatment (Yuan et al., 2018). These studies suggest the possible function of PERK in regulating tau pathology.

To further investigate how PERK regulates tau, we postulated that manipulation of PERK activity will result in differential tau protein aggregation behavior, alleviating or worsening tau protein aggregation. To test this, we employed a cell culture method developed by Marc Diamond's team (2014) to study tau aggregation. They engineered a "biosensor" HEK293T cell line to express a human tau repeat domain (TauRD) with tauopathy associated P301S mutation fused to YFP and named this system as "tau biosensor cells" (Holmes et al., 2014). The YFP fluorescence signal thus reliably revealed tau reporter protein (TauRD-YFP) aggregation. They successfully quantified tau seeding activity under tauopathy disease progression and found a robust seeding activity of tau before the earliest histopathological stain of tauopathy (Holmes et al., 2014). We obtained these biosensor cells from the Marc Diamond lab to study tau protein

aggregation in cell culture. We pharmacologically manipulated PERK activity using PERK inhibitors (GSK2606414, GSK2656157, ISRIB) or PERK pathway activator (salubrinal) on such reliable tau biosensor cells and examined the formation of YFP fluorescent puncta under the microscopy. We then quantified the number of TauRD-YFP puncta in the tau biosensor cells after treatment with different PERK pathway drugs.

3.2 Materials and Method

Cell Culture and Cell Line

A previously published biosensor cell line that derived from HEK cell line, expressing a 4R tau repeat domain with P301S mutation fused with yellow fluorescent protein (TauRD(P301S)-YFP) was provided by Marc Diamond's team. All cells were grown in complete media (DMEM (Gibco 11-965-118) +10% FBS+ 1% penicillin/streptomycin). After cells reach over 90% cell confluency and attach to the bottom of the plate, cell growing media was sucked out and washed with 5mL DPBS. Then, 1mL Trypsin was added to the plate to dissociate the cells from the bottom, followed by 5min incubation at 37℃ incubator. After incubation, cells were harvest by adding 9mL media and transferred to a vial tube for 2-3mins centrifuge at 2000rpm speed. Supernatant was later sucked out and replaced with 10mL fresh media. After thorough mixing, 1mL of the mixture was added to a new plate with 12mL new media for 1:10 dilution. The whole process was repeated for maintaining the biosensor HEK293 cell culture.

Liposome-Mediated Transduction of Tau Seeds and pharmacological treatment

Biosensor cells were plated at a density of 5,000 cells per well in a 12-well plate. We kept a low cell density for allowing aggregation of tau seeds (PS19 hTau transgenic mouse brain lysates), which requires at least 24 hour incubation time. After culturing overnight, cells were transduced with PS19 brain lysate at above 80% confluency. TransIT-LT1 reagent was warmed to room temperature and gently vortexed. 100µL Opti-MEM medium was placed in a sterile tube. 1ug/µL PS19 brain lysate is later added to the sterile tube, followed by gentle mixing by pipetting. Then, 3µL TransIT-LT1 transfection reagent (Mirus co) is added, followed by gentle mixing by pipetting. Liposome preparations were incubated at room temperature for 20 min before adding to cells. Subsequently, liposome transduction reagent is added dropwise to each

well to make up to a total volume of 1mL per well. Cells are then transferred to 37℃ incubator for incubation. 24hr after transduction, chemical compounds of PERK inhibitors (GSK2606414: Tocris 5197; GSK2656157: Selleckchem S7033; ISRIB: Sigma SML0843), IRE1 inhibitor (4u8c: Selleckchem S7272), ATF6 inhibitor (Ceapin-A7: Sigma SML2330) and GADD34 inhibitor (Salubrinal: Selleckchem S2923; Sephin-1: Selleckchem S6391), are added to the plate at the desired concentration and incubated at 37℃ incubator for 24hr. The desired concentration was determined by pretesting of toxic and effective doses.

Confocal microscopy

Cell plates pretreated with ER stress compounds were incubated for 2~4 days to form Tau aggregation. The YFP imaging was performed with Leica SP8 confocal microscope and Zeiss LSM710 Zen Black confocal microscope at 10x (4x magnification) resolution. Image frame size: 1024x1024; Scan Speed 6; Data Depth 16 bit; z-stack: 3um/ 5 slices. Images were analyzed by using FIJI and the cell counter plug-in scored aggregate morphology in terms of the number of aggregates that stand out from the whole cell population.

Statistical Analysis

All the statistics were expressed as mean ± standard error of the mean (SEM). Student's t-test was used for comparison. Two-way ANOVA and Fisher's least significant difference procedure (LSD test) were used to examine the differences among the group of means. All the statistical tests were performed using GraphPad Prism 6. The difference between the means of separate experimental groups was considered statistically significant at $P < 0.05$.

3.3 Results

PERK pathway activity prevents tau-YFP aggregation

To understand the physiological behavior of tau-YFP in BioSensor cells, we transiently transfected PS19 tauopathy mouse brain lysate into biosensor cells endogenously expressing the TauRD(P301S)-YFP, which is invented by Marc Diamond's group. The TauRD fragment tagging with yellow fluorescent protein (YFP) signal detected under the confocal microscope reliably represents the aggregation of tau. We measured the tau aggregation in both dose-dependent (Figure 13a and 13b) and time-dependent manner (Figure 12a and 12b). The confocal microscopy image and the quantification confirms both dose-dependent and time dependent increase of tau aggregates under PS19 control experiment group, indicating the accumulation of the Tau-YFP after the PS19 mouse brain lysate transfection (Figure 12 and 13).

To further assess how manipulation of PERK activity will affect tau seeding, we conducted pharmacological modulation on the above-mentioned transfected biosensor cells. To specify, two direct PERK inhibitors, GSK2656157 and GSK2606414, and an integrated stress response (ISR) inhibitor targeting eIF2B to reverse the effect of eIF2α phosphorylation, ISRIB are used to inhibit PERK pathway activity (Figure 14c). Salubrinal, a selective eIF2α phosphatase, GADD34, inhibitor is used to enhance PERK pathway activity (Figure 14c). Tau biosensor cells transiently transfected with wild-type mouse brain lysate (no human tau) serves as a negative control while PS19 mice brain lysate (containing human Tau P301S) serves as a positive control. The confocal microscopy image confirms the presence of tau-YFP aggregates in tauopathy brain lysate in comparison to no presence of tau-YFP aggregates after WT brain lysate (Figure 14a and 14b). Inhibition of PERK activity by either GSK2656157, GSK2606414 or ISRIB all increased the number of tau-YFP aggregates significantly (Figure 14a and 14b). On the

other hand, salubrinal caused a significant decrease of tau-YFP aggregates(Figure 14a and 14b). Altogether, we could conclude that PERK activity prevents tau-YFP aggregation in biosensor cells, and inhibition of PERK activity promoted tau-YFP aggregation in Biosensor cells. Based on this, we propose that PERK activity has a protective effect on regulating tau accumulation.

3.4 Discussion

In the biosensor cell experiment, we found that Tau P301S PS19 mouse protein lysates lead to increase in tau-YFP aggregation in biosensor cells (Figure 12 and 13). We found that pharmacochemical modulation of the PERK pathway can change the number tau-YFP aggregates in biosensor cells (Figure 13). For pharmacochemical modulation, we utilized four chemicals, GSK2606414, GSK2656157, ISRIB, and salubrinal. GSK2606414 and GSK2656157 are ATP-competitive inhibitor of PERK enzymatic activity, inhibiting PERK autophosphorylation and eIF2α substrate phosphorylation (Atkins *et al.*, 2013). ISRIB, on the other hand, facilitates the assembly of eIF2B and reverses the effect of eIF2α phosphorylation (Rabouw *et al.*, 2019). Hence, both GSK2606414, GSK2656157 and ISRIB act as PERK inhibitors that lead to translational attenuation. When we treated the biosensor cells with either of these three inhibitors, we observed an increase in the number of tau seeds in our biosensor cells experiment (Figure 14b and 14c).

Different from the two PERK inhibitors, salubrinal is an inhibitor for GADD34, the eIF2α phosphatase; it is known to attenuate the activation of PERK(Gupta *et al.*, 2019). Thus, salubrinal acts as a PERK pathway activator because it enhances phosphor-eIF2a levels thereby promoting translational attenuation. Salubrinal has shown its protective effect in multiple studies. In particular, there is evidence for reduced DNA damage and neuronal apoptosis as well as extending the life span of transgenic mice in Parkinson's disease (Gupta *et al.*, 2019; Colla *et al.*, 2012). In our studies, we found a significantly decreased number of tau-YFP aggregates in salubrinal treated Biosensor cells (Figure 14b and 14c). As a result, we conclude that our experiment shows that PERK activity prevents tau-YFP aggregation. It also suggests that salubrinal may be a good drug to limiting tauopathy disease progression in PSP.

Since many downstream targets of PERK-eIF2α pathway, including translation initiation, ATF4, and CHOP, are crucial players of the pathway, it is possible that the synergistic effects of all downstream targets or any related alternative pathways triggered by them are responsible for the change in tau aggregation. Altered expression of those downstream targets or altered activation of their related pathways in response to pharmacochemical modulation could positively or negatively act on translation. Therefore, future experiments can use other chemicals that act on both eIF2α and its downstream targets to fully understand the PERK-eIF2α pathway. Experiments to test chemicals that activate or inhibit other UPR pathways suchas IRE1 and ATF6 may also be informative.

3.5 Figures and Tables

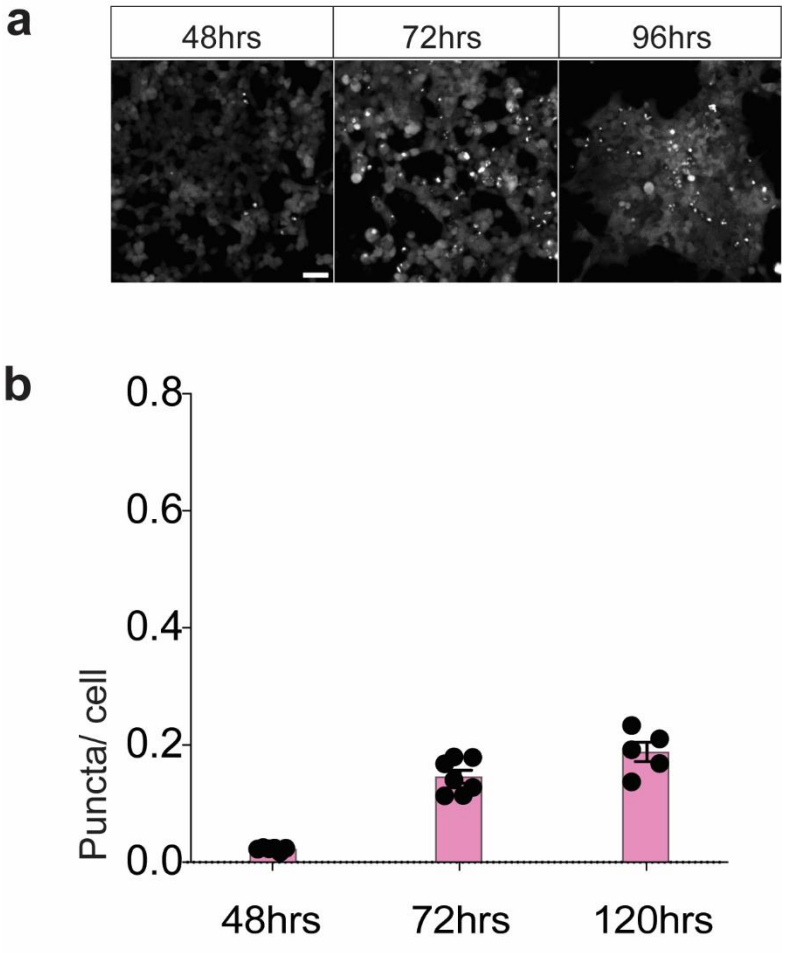

Figure 12. Fluorescent tau aggregates increase with time in PS19 tauopathy mouse brain lysates transfected TauRD-YFP biosensor cells.
(a) Confocal microscopic image of tau aggregates at 48hrs, 72 hrs and 96hrs after transfection. Tau aggregates are shown in white. (b) Quantified graph of relative number of puncta (tau aggregates) observed over total number of cells present at 48hrs, 72 hrs and 96hrs after transfection.

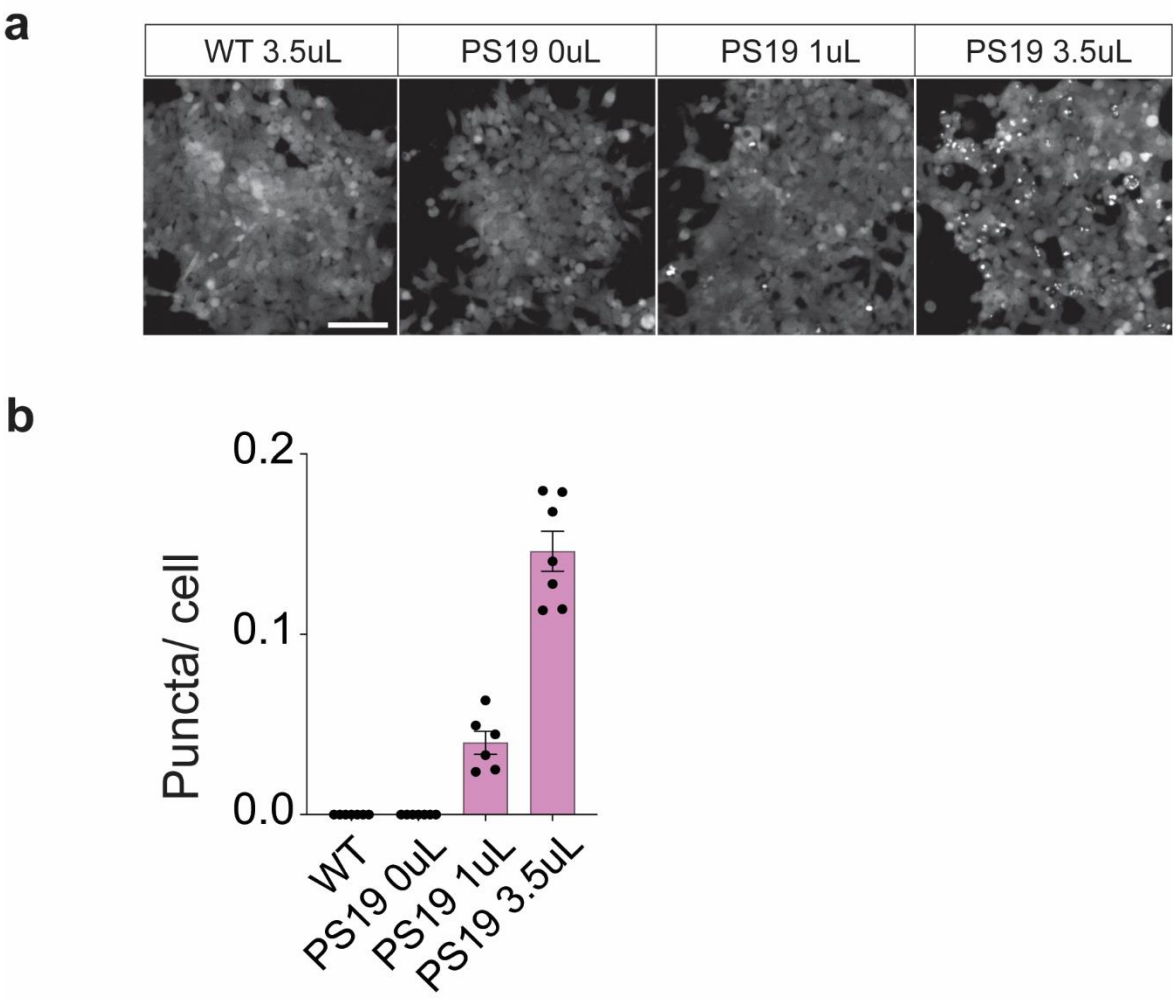

Figure 13. Fluorescent tau aggregates increase in TauRD-YFP biosensor cells transfected with increasing concentration of PS19 tauopathy brain lysates.

(a) Confocal microscopic image of tau aggregatesin TaRD-YFP biosensor cells transfected with 0µL, 1µL and 3.5µL PS19 brain lysates. Tau aggregates are shown in white. (b) Quantified graph of relative number of puncta (tau aggregates) observed over total number of cells present at three concentrations.

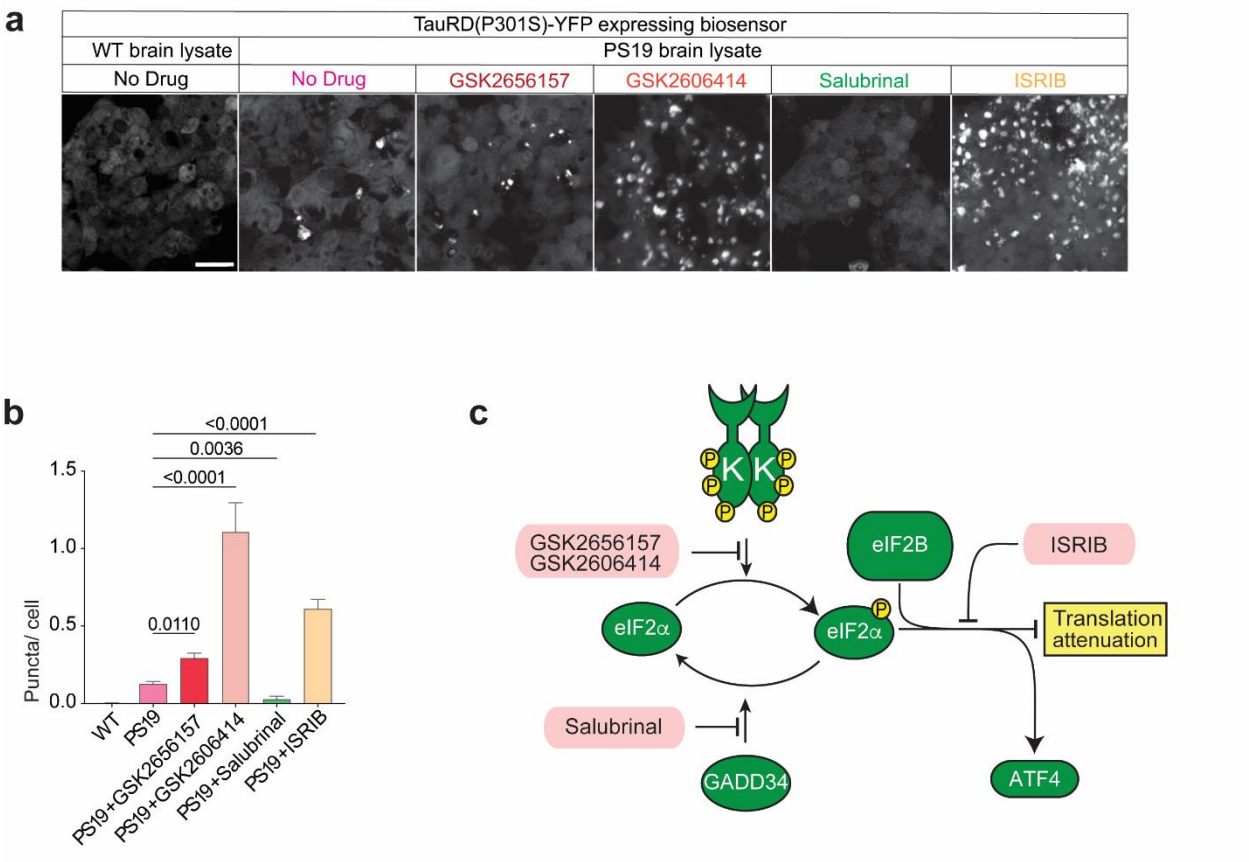

Figure 14. TauRD-YFP aggregation changes upon pharmacochemical modulation of PERK activity.

(a) Confocal microscopic image of no drug treated WT brain lysate transfected TauRD-YFP biosensor cells control as well as either no drug or drug treated tauopathy brain lysates transfected TauRD-YFP biosensor cells. Tau aggregates are shown in white. (b) Quantified graph of relative number of puncta (tau aggregates) observed over total number of cells present at conditions in (a). (c) Diagram showing mechanisms of four chemicals we used. GSK2656157 and GSK2606414 inhibit PERK autophosphorylation and eIF2α substrate phosphorylation. ISRIB facilitates the assembly of eIF2B and reverses the effect of eIF2α phosphorylation. All three lead to translational attenuation. Salubrinal is an inhibitor for eIF2α phosphatase, GADD 34, inhibiting the translational attenuation.

The experiments and figures in Chapter 3 were performed/created with Dr. GoonHo Park. The thesis author was the primary author of this chapter.

References

Alzheimer's Association (2016). 2016 Alzheimer's disease facts and figures. Alzheimer's & dementia : the journal of the Alzheimer's Association, 12(4), 459–509.

Alzheimer's disease facts and figures. (2020). Alzheimer's & dementia : the journal of the

Alyenbaawi, H., Allison, W. T., & Mok, S. A. (2020). Prion-Like Propagation Mechanisms in Tauopathies and Traumatic Brain Injury: Challenges and Prospects. Biomolecules, 10(11), 1487.

Atkins, C., Liu, Q., Minthorn, E., Zhang, S. Y., Figueroa, D. J., Moss, K., Stanley, T. B., Sanders, B., Goetz, A., Gaul, N., Choudhry, A. E., Alsaid, H., Jucker, B. M., Axten, J. M., & Kumar, R. (2013). Characterization of a novel PERK kinase inhibitor with antitumor and antiangiogenic activity. Cancer research, 73(6), 1993–2002.

Ballatore, C., Lee, V. M., & Trojanowski, J. Q. (2007). Tau-mediated neurodegeneration in Alzheimer's disease and related disorders. Nature reviews. Neuroscience, 8(9), 663–672.

Bell, M. C., Meier, S. E., Ingram, A. L., & Abisambra, J. F. (2016). PERK-opathies: An Endoplasmic Reticulum Stress Mechanism Underlying Neurodegeneration. Current Alzheimer research, 13(2), 150–163.

Braak, H., & Braak, E. (1991). Neuropathological stageing of Alzheimer-related changes. Acta neuropathologica, 82(4), 239–259.

Colla, E., Jensen, P. H., Pletnikova, O., Troncoso, J. C., Glabe, C., & Lee, M. K. (2012). Accumulation of toxic α-synuclein oligomer within endoplasmic reticulum occurs in α-synucleinopathy in vivo. The Journal of neuroscience : the official journal of the Society for Neuroscience, 32(10), 3301–3305.

Congdon, E. E., & Sigurdsson, E. M. (2018). Tau-targeting therapies for Alzheimer disease. Nature reviews. Neurology, 14(7), 399–415.

Dickson, D.W., Rademakers, R. and Hutton, M.L. (2007), Progressive Supranuclear Palsy: Pathology and Genetics. Brain Pathology, 17: 74-82.

Erkkinen, M. G., Kim, M. O., & Geschwind, M. D. (2018). Clinical Neurology and Epidemiology of the Major Neurodegenerative Diseases. Cold Spring Harbor perspectives in biology, 10(4), a033118.

Espinoza, M., de Silva, R., Dickson, D. W., & Davies, P. (2008). Differential incorporation of tau isoforms in Alzheimer's disease. Journal of Alzheimer's disease : JAD, 14(1), 1–16.

Ferrari, R., Ryten, M., Simone, R., Trabzuni, D., Nicolaou, N., Hondhamuni, G., Ramasamy, A., Vandrovcova, J., UK Brain Expression Consortium, Weale, M. E., Lees, A. J., Momeni,

P., Hardy, J., & de Silva, R. (2014). Assessment of common variability and expression quantitative trait loci for genome-wide associations for progressive supranuclear palsy. Neurobiology of aging, 35(6), 1514.e1–1514.e12.

Frost, B., Jacks, R. L., & Diamond, M. I. (2009). Propagation of tau misfolding from the outside to the inside of a cell. The Journal of biological chemistry, 284(19), 12845–12852.

Ganguly, G., Chakrabarti, S., Chatterjee, U., & Saso, L. (2017). Proteinopathy, oxidative stress and mitochondrial dysfunction: cross talk in Alzheimer's disease and Parkinson's disease. Drug design, development and therapy, 11, 797–810.

Gardner, B. M., Pincus, D., Gotthardt, K., Gallagher, C. M., & Walter, P. (2013). Endoplasmic reticulum stress sensing in the unfolded protein response. Cold Spring Harbor perspectives in biology, 5(3), a013169.

Ghemrawi R, Khair M. Endoplasmic Reticulum Stress and Unfolded Protein Response in Neurodegenerative Diseases. Int J Mol Sci. 2020 Aug 25;21(17):6127. doi: 10.3390/ijms21176127. PMID: 32854418; PMCID: PMC7503386.

Gitler, A. D., Dhillon, P., & Shorter, J. (2017). Neurodegenerative disease: models, mechanisms, and a new hope. Disease models & mechanisms, 10(5), 499–502.

Goedert, M., Spillantini, M. G., Cairns, N. J., & Crowther, R. A. (1992). Tau proteins of Alzheimer paired helical filaments: abnormal phosphorylation of all six brain isoforms. Neuron, 8(1), 159–168.

Gupta, S., Biswas, J., Gupta, P., Singh, A., Tiwari, S., Mishra, A., & Singh, S. (2019). Salubrinal attenuates nitric oxide mediated PERK:IRE1α: ATF-6 signaling and DNA damage in neuronal cells. Neurochemistry international, 131, 104581.

Hetz, C., & Saxena, S. (2017). ER stress and the unfolded protein response in neurodegeneration. Nature reviews. Neurology, 13(8), 477–491.

Hiramatsu, N., Chiang, W. C., Kurt, T. D., Sigurdson, C. J., & Lin, J. H. (2015). Multiple Mechanisms of Unfolded Protein Response-Induced Cell Death. The American journal of pathology, 185(7), 1800–1808.

Höglinger, G. U., Melhem, N. M., Dickson, D. W., Sleiman, P. M., Wang, L. S., Klei, L., Rademakers, R., de Silva, R., Litvan, I., Riley, D. E., van Swieten, J. C., Heutink, P., Wszolek, Z. K., Uitti, R. J., Vandrovcova, J., Hurtig, H. I., Gross, R. G., Maetzler, W., Goldwurm, S., Tolosa, E., Schellenberg, G. D. (2011). Identification of common variants influencing risk of the tauopathy progressive supranuclear palsy. Nature genetics, 43(7), 699–705.

Holmes, B. B., Furman, J. L., Mahan, T. E., Yamasaki, T. R., Mirbaha, H., Eades, W. C., Belaygorod, L., Cairns, N. J., Holtzman, D. M., & Diamond, M. I. (2014). Proteopathic

tau seeding predicts tauopathy in vivo. Proceedings of the National Academy of Sciences of the United States of America, 111(41), E4376–E4385.

Hoozemans, J. J., Veerhuis, R., Van Haastert, E. S., Rozemuller, J. M., Baas, F., Eikelenboom, P., & Scheper, W. (2005). The unfolded protein response is activated in Alzheimer's disease. Acta neuropathologica, 110(2), 165–172.

Iba, M., Guo, J. L., McBride, J. D., Zhang, B., Trojanowski, J. Q., & Lee, V. M. (2013). Synthetic tau fibrils mediate transmission of neurofibrillary tangles in a transgenic mouse model of Alzheimer's-like tauopathy. The Journal of neuroscience : the official journal of the Society for Neuroscience, 33(3), 1024–1037.

Kametani, F., & Hasegawa, M. (2018). Reconsideration of Amyloid Hypothesis and Tau Hypothesis in Alzheimer's Disease. Frontiers in neuroscience, 12, 25.

Liu, Z., Lv, Y., Zhao, N., Guan, G., & Wang, J. (2015). Protein kinase R-like ER kinase and its role in endoplasmic reticulum stress-decided cell fate. Cell death & disease, 6(7), e1822.

Lunenfeld, B., & Stratton, P. (2013). The clinical consequences of an ageing world and preventive strategies. Best practice & research. Clinical obstetrics & gynaecology, 27(5), 643–659.

Meyer-Luehmann, M., Coomaraswamy, J., Bolmont, T., Kaeser, S., Schaefer, C., Kilger, E., Neuenschwander, A., Abramowski, D., Frey, P., Jaton, A. L., Vigouret, J. M., Paganetti, P., Walsh, D. M., Mathews, P. M., Ghiso, J., Staufenbiel, M., Walker, L. C., & Jucker, M. (2006). Exogenous induction of cerebral beta-amyloidogenesis is governed by agent and host. Science (New York, N.Y.), 313(5794), 1781–1784.

Nagasawa, I., Kunimasa, K., Tsukahara, S., & Tomida, A. (2017). BRAF-mutated cells activate GCN2-mediated integrated stress response as a cytoprotective mechanism in response to vemurafenib. Biochemical and biophysical research communications, 482(4), 1491–1497.

Rabouw, H. H., Langereis, M. A., Anand, A. A., Visser, L. J., de Groot, R. J., Walter, P., & van Kuppeveld, F. (2019). Small molecule ISRIB suppresses the integrated stress response within a defined window of activation. Proceedings of the National Academy of Sciences of the United States of America, 116(6), 2097–2102.

Ron, D., & Walter, P. (2007). Signal integration in the endoplasmic reticulum unfolded protein response. Nature reviews. Molecular cell biology, 8(7), 519–529.

Rothe, S., Prakash, A., & Tyedmers, J. (2018). The Insoluble Protein Deposit (IPOD) in Yeast. Frontiers in molecular neuroscience, 11, 237. https://doi.org/10.3389/fnmol.2018.00237

Saha, P., & Sen, N. (2019). Tauopathy: A common mechanism for neurodegeneration and brain aging. Mechanisms of ageing and development, 178, 72–79.

Sakae, N., Josephs, K. A., Litvan, I., Murray, M. E., Duara, R., Uitti, R. J., Wszolek, Z. K., Graff-Radford, N. R., & Dickson, D. W. (2019). Neuropathologic basis of frontotemporal dementia in progressive supranuclear palsy. Movement disorders : official journal of the Movement Disorder Society, 34(11), 1655–1662.

Sanchez-Contreras, M. Y., Kouri, N., Cook, C. N., Serie, D. J., Heckman, M. G., Finch, N. A., Caselli, R. J., Uitti, R. J., Wszolek, Z. K., Graff-Radford, N., Petrucelli, L., Wang, L. S., Schellenberg, G. D., Dickson, D. W., Rademakers, R., & Ross, O. A. (2018). Replication of progressive supranuclear palsy genome-wide association study identifies SLCO1A2 and DUSP10 as new susceptibility loci. Molecular neurodegeneration, 13(1), 37.

Schöll, M., Maass, A., Mattsson, N., Ashton, N. J., Blennow, K., Zetterberg, H., & Jagust, W. (2019). Biomarkers for tau pathology. Molecular and cellular neurosciences, 97, 18–33.

Silva, M. C., & Haggarty, S. J. (2020). Tauopathies: Deciphering Disease Mechanisms to Develop Effective Therapies. International journal of molecular sciences, 21(23), 8948.

Stoothoff, W. H., & Johnson, G. V. (2005). Tau phosphorylation: physiological and pathological consequences. Biochimica et biophysica acta, 1739(2-3), 280–297.

Stutzbach, L. D., Xie, S. X., Naj, A. C., Albin, R., Gilman, S., PSP Genetics Study Group, Lee, V. M., Trojanowski, J. Q., Devlin, B., & Schellenberg, G. D. (2013). The unfolded protein response is activated in disease-affected brain regions in progressive supranuclear palsy and Alzheimer's disease. Acta neuropathologica communications, 1, 31.

Takalo, M., Salminen, A., Soininen, H., Hiltunen, M., & Haapasalo, A. (2013). Protein aggregation and degradation mechanisms in neurodegenerative diseases. American journal of neurodegenerative disease, 2(1), 1–14.

Takeda S. (2019). Progression of Alzheimer's disease, tau propagation, and its modifiable risk factors. Neuroscience research, 141, 36–42.

Wang, Y., & Mandelkow, E. (2016). Tau in physiology and pathology. Nature reviews. Neuroscience, 17(1), 5–21.

Wong, T. H., van der Lee, S. J., van Rooij, J., Meeter, L., Frick, P., Melhem, S., Seelaar, H., Ikram, M. A., Rozemuller, A. J., Holstege, H., Hulsman, M., Uitterlinden, A., Neumann, M., Hoozemans, J., van Duijn, C. M., Rademakers, R., & van Swieten, J. C. (2019). EIF2AK3 variants in Dutch patients with Alzheimer's disease. Neurobiology of aging, 73, 229.e11–229.e18.

Yuan, S. H., Hiramatsu, N., Liu, Q., Sun, X. V., Lenh, D., Chan, P., Chiang, K., Koo, E. H., Kao, A. W., Litvan, I., & Lin, J. H. (2018). Tauopathy-associated PERK alleles are functional hypomorphs that increase neuronal vulnerability to ER stress. Human molecular genetics, 27(22), 3951–3963.